Electroendocytosis: Exposure of Cells to Pulsed Low Electric Fields Enhances Adsorption and Uptake of Macromolecules

Yulia Antov, Alexander Barbul, Hila Mantsur, and Rafi Korenstein
Department of Physiology and Pharmacology, Sackler Faculty of Medicine, Tel Aviv University, Tel Aviv, Israel

ABSTRACT This study demonstrates alteration of cell surface, leading to enhanced adsorption of macromolecules (bovine serum albumin (BSA), dextran, and DNA), after the exposure of cells to unipolar pulsed low electric fields (LEF). Modification of the adsorptive properties of the cell membrane also stems from the observation of LEF-induced cell-cell aggregation. Analysis of the adsorption isotherms of BSA-fluorescein isothiocyanate (FITC) to the surface of COS 5-7 cells reveals that the stimulated adsorption can be attributed to LEF-induced increase in the capacity of both specific and nonspecific binding. The enhanced adsorption was consequently followed by increased uptake. At 20 V/cm the maximal binding and subsequent uptake of BSA-FITC attached to specific sites are 6.5- and 7.4-fold higher than in controls, respectively. The nonspecific LEF-induced binding and uptake of BSA are 34- and 5.2-fold higher than in controls. LEF-enhanced adsorption is a temperature-independent process, whereas LEF-induced uptake is a temperature-dependent one that is abolished at 4°C. The stimulation of adsorption and uptake is reversible, revealing similar decay kinetics at room temperature. It is suggested that electrophoretic segregation of charged components in the outer leaflet of the cell membrane is responsible for both enhanced adsorption and stimulated uptake via changes of the membrane elastic properties that enhance budding and fission processes.

INTRODUCTION

Studies of electric field effects on cells have been carried out in three major domains of high, low, and extremely low electric fields. The application of high-pulsed electric fields to cells, leading to the induction of a transmembrane potential difference $>\sim$200 mV, has been associated mostly with the phenomenon of electroporation (Neumann and Rosenheck, 1972; Zimmermann et al., 1974; Kinosita and Tsong, 1977). Its employment has gained wide use in the areas of cell biology and biotechnology, since it supplied an efficient physical tool to permeabilize cells by opening hydrophilic pathways in the cell membrane, through which molecules could diffuse along their electrochemical gradients (for recent reviews, see Teissie, 2002; Weaver, 2003; Gehl, 2003). Exposure of cells to extremely low electric and magnetic fields, which can induce a transmembrane potential difference $<$1 mV, have been associated with environmental exposures of humans to low-frequency electromagnetic fields on the one hand, and, on the other, with possible application of medical therapeutic devices (for reviews, see Lacy-Hulbert et al., 1998; Adair, 1999; Ahlbom et al., 2001). The underlying mechanisms of these very weak electric fields are still ill understood and highly debated (Adair, 1999; Weaver et al., 1999, 2000; Foster, 2003). The intermediate domain of low electric fields, which may lead to the induction of transmembrane potential alteration in the range of 1–100 mV, has been routinely applied in electrophysiological studies of ion transport through channels. It was realized quite early that physiological electric fields in tissues are at the lower end of this range (Jaffe, 1966; Nuccitelli and Jaffe, 1974; Borgens et al., 1977). These endogenous electric fields were associated with processes of development, regeneration and wound healing (Nuccitelli, 2003). An attempt was made to understand the role of these electric fields under situations imitating physiological and pathological conditions by applying low DC electric fields and examining the phenomenon of electrophoresis of charged membrane components in the plane of the cell membrane. Lateral electrophoretic displacements of charged membrane proteins and lipids resulted in segregation of these components at the cell surface (Poo and Robinson, 1977; Poo et al., 1979; Poo, 1981). Recent studies of the effect of low DC electric fields on altering basic cellular activities such as cell cycle, directional growth, and motility explored the underlying cellular pathways involved in inducing these changes (e.g., Zhao et al., 2002; Song et al., 2002; Wang et al., 2003).

An additional manifestation of the possibility to affect natural cellular functions by low electric fields emerges from our previous observation that exposure of cells to pulsed low electric fields can stimulate endocytic activity (Rosemberg and Korenstein, 1997). We could demonstrate the enhanced uptake of macromolecules (polysaccharides in the range of 1–2000 kD and β-galactosidase) via stimulating endocytic-like processes by exposing cells to a train of pulsed low electric fields (LEF). Recently, we have extended this study by exploring the basic spatial and time-dependent characteristics of LEF-induced uptake via adsorptive and fluid-phase uptake (Antov et al., 2004).

Submitted August 12, 2004, and accepted for publication October 22, 2004.

Yulia Antov and Alexander Barbul contributed equally to this work.

Address reprint requests to Prof. Rafi Korenstein, Dept. of Physiology and Pharmacology, Sackler School of Medicine, Tel Aviv University, Tel Aviv 69978, Israel. Tel.: 972-3-640-6042; Fax: 972-3-640-8982; E-mail: korens@post.tau.ac.il.

0006-3495/05/03/2206/18 $2.00

doi: 10.1529/biophysj.104.051268

In this study we explore the steady-state and temporal LEF-induced changes in the adsorption properties of the cell surface and the interrelationship of these changes with the subsequently enhanced uptake process.

MATERIALS AND METHODS

Cell culture

COS 5-7 (fibroblast-like cells, African green monkey kidney derived from CV-1 subclone of COS 7) were cultured in Dulbecco's modified Eagle's medium (DMEM) supplemented with L-glutamine (2 mM), 10% fetal calf serum (FCS), and 0.05% PSN solution (penicillin 10.000 units/ml, streptomycin 10 mg/ml, and nystatin 1250 units/ml). HaCaT cells (human keratinocyte cell line, gift from Prof. N. E. Fusenig of Deutsches Krebsforschungszentrum, Heidelberg) were cultured in MEM-NAA medium supplemented with L-glutamine (2 mM), 5% FCS, and 0.05% PSN solution. All cells were grown in 75-cm^2 tissue culture flasks (Corning, Corning, NY) at 37°C, in a humid atmosphere of 5% CO_2 in air. Cells were harvested at the log phase of growth by trypsinization (0.25% trypsin and 0.05% EDTA) for 5 min at 37°C. After washing twice by centrifugation (5 min, 210 × *g*; RT6000D, Sorvall, Asheville, NC), cells were resuspended ($1–10 \times 10^6$ cells/ml) in exposure medium (in most cases serum-free DMEM without phenol red, supplemented with 25 mM Hepes (DMEM-H)). All culture media, antibiotics, trypsin, and FCS were purchased from Biological Industries (Beth Haemek, Israel).

Exposure of cells to pulsed electric fields

Cells in suspension were exposed to a train of low intensity unipolar rectangular voltage pulses by employing an electric pulse generator (Grass S44 Stimulator, Grass-Telefactor, West Warwick, RI). The exposure was performed in a plastic cuvette by placing the cell suspension between two parallel stainless steel electrodes separated by 0.5 cm, yielding a uniform electric field. The electric field parameters were monitored on line by recording voltage and current (using a wide-band current transformer, Rearson Electronics, Palo Alto, CA) on a Tektronix 2430A oscilloscope (Tektronix, Beaverton, OR). Experiments were run at different temperatures in the range of 4–37°C. In routine experiments, 0.5 ml of cell suspension ($0.5–10 \times 10^6$ cells/ml) in DMEM-H was exposed to a train of electric field pulses of 20 V/cm. The train consisted of unipolar rectangular pulses of 180 μs duration, frequency of 500 Hz, and total exposure time of 1 min. The application of this train of pulses resulted in small polarization of the electrodes and the appearance of a residual low DC component ($\leq$2 V) at the highest electric field. The temperature of the solutions during exposure was measured using fiberoptic temperature sensors (FISO Technologies, Quebec, Canada). The readings were recorded every 2.2 s with averaging 1 s/point. The typical transient temperature rise measured at the end of 1 min exposure in DMEM-H medium to LEF of 20 V/cm at 4°C, 24°C, and 37°C was 1.4 ± 0.6°C.

Molecular probes

Dextran conjugated to fluorescein-5-isothiocyanate (dextran-FITC, 2000 kDa, 0.009 mol FITC/mole glucose) was used at a final concentration of 0.2 μM. Bovine serum albumin conjugated to fluorescein-5-isothiocyanate (BSA-FITC) contained 12 mol FITC per mole albumin (66 kDa). Both FITC-conjugated probes were dialyzed before use against the exposure medium. Propidium iodide (PI) was used at the final concentration of 30 μM for the detection of damaged cells. These markers were purchased from Sigma Chemicals (Rehovot, Israel). No change was detected in the fluorescent spectra of the different probes at the specified concentration used, suggesting that no probe aggregation took place under the conditions employed.

Measurement of adsorption and uptake by flow cytometry, fluorimetry, and confocal fluorescence microscopy

Cells (usually 3×10^6 ml^{-1}) were exposed to low electric fields in the presence of a molecular probe. In some cases the probes were added after the exposure of the cells to LEF. After exposure and incubation with the probe, cells were washed twice in DMEM-H medium. Since BSA-FITC was found to be significantly adsorbed to the cell membrane, especially after exposure to LEF, we differentiated between internalized and adsorbed fractions of the probe by subjecting the cells to 0.01% trypsin in phosphate-buffered solution for 5 min at 37°C (Glogauer, 1992). The trypsin-digested BSA-FITC represents the amount of BSA adsorbed to the cell population, whereas the amount of the probe measured per single cell is attributed to the internalized amount of the probe. The efficiency of removal of the adsorbed BSA-FITC probe from the cell surface by trypsin was validated by confocal fluorescence microscopy (LSM 410, Zeiss, Jena, Germany). To visualize the cellular location of the probe the exposed cell suspensions and controls were washed twice in DMEM-H and kept at the chosen temperature, until observation at the appropriate time by confocal microscopy. Computer-generated images of 0.5-μm optical sections were obtained at the approximate geometric center of the cell as determined by repeated optical sectioning.

Flow cytometry analysis was carried out by FACSort (Becton Dickinson, San Jose, CA), employing 488-nm argon laser excitation. The green fluorescence of FITC was measured via 530/30-nm filter whereas the red fluorescence of PI was detected via 585/42-nm filter. To eliminate signals due to cellular fragments, only those events with forward and side light scattering comparable to whole cells were analyzed. The side light scattering was also employed to detect changes in the formation or disappearance of intracellular vesicles. All fluorescence signals were logarithmically displayed. Ten thousand cells were run for each sample and data were collected in the list mode. The analysis of flow cytometry data was performed using WINMDI 2.8 flow cytometry application software. Control samples exhibited a rise in fluorescence when incubated with fluorescent probes at 24°C due to constitutive uptake. Cells exposed to LEF without any probe also revealed an increased fluorescence as compared to untreated control cells due to a rise in autofluorescence after exposure. This background signal was subtracted from the fluorescence of all cells exposed to electric field. Results were expressed in terms of cell quantities at 95% confidence interval or as the geometric mean of cell population. The geometric mean (G_m) was used for log-amplified data as it takes into account the weighting of data distribution. The combined LEF-induced adsorption and uptake of the probe was determined by flow cytometry of cells that were not subjected to the trypsinization step (Fig. 1 *J*, histogram *3*). In contrast, the uptake of the probe was determined by flow cytometry of cells after being subjected to trypsinization (Fig. 1 *J*, histogram *4*). Efficiencies of probe adsorption and uptake were characterized by fold of induction (FI) which was calculated as a ratio of the geometric mean of fluorescence in an exposed sample to that of a control unexposed one.

A direct measurement of the amount of BSA-FITC adsorbed to the cells was carried out by measuring the fluorescence of the probe in the extracellular medium, after the release of fragmented BSA-FITC from the cell surface after trypsinization. FITC fluorescence was measured using a microplate fluorescence reader (FL-600, Bio-tek, Winooski, VT; $\lambda_{ex} = 485/20$, $\lambda_{em} = 530/25$). The readings were normalized to the fraction removed from the unexposed samples.

Cell viability was assessed by the propidium iodide exclusion test. For flow cytometry and confocal microscopy, PI (30 μM) was added to exposed and control cells 5 min before evaluation.

Binding and uptake studies

The adsorption of albumin to the plasma membrane of COS 5-7 cells was characterized using BSA-FITC as a probe. The cells were washed three

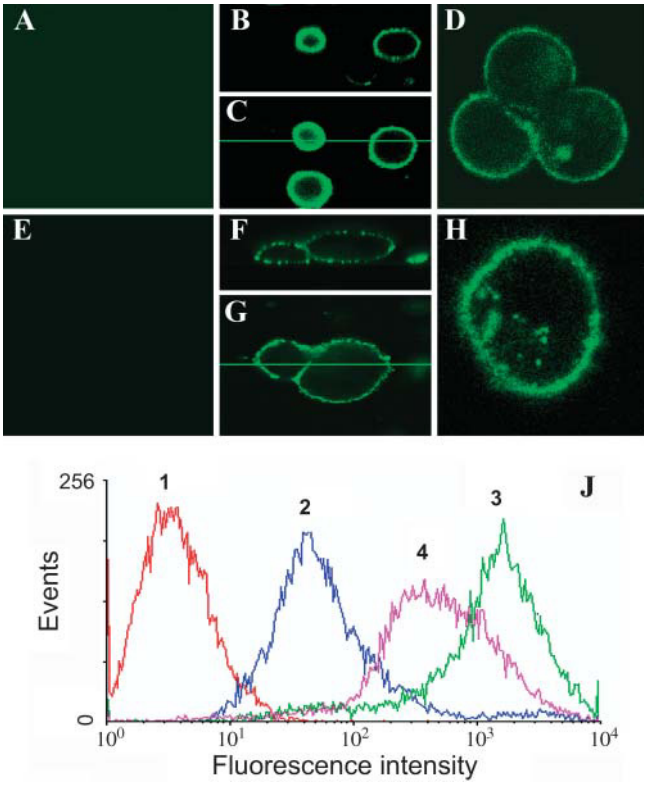

FIGURE 1 Low electric field-stimulated adsorption of dextran-FITC (*A–D*) and BSA-FITC (*E–H*) to the plasma membrane of COS 5-7 cells. Cell suspensions of COS 5-7 cells in DMEM-H were preincubated at 4°C with 0.2 μM of dextran-FITC or 6.8 μM BSA-FITC for 4 min, subjected to LEF treatment of 20 V/cm for 1 min, and followed by three successive washings with DMEM solution at 4°C. Immediately after the last wash, cells were subjected to analysis by confocal microscopy (LSM 410, Zeiss). (*A* and *E*) Confocal horizontal optical sections of FITC fluorescence taken at center of control unexposed cells incubated with dextran-FITC and BSA-FITC, respectively. (*C* and *G*) Optical central sections through the horizontal plane of exposed cells. (*B* and *F*) Corresponding optical sections through the vertical plane. Increasing the temperature of the exposed cells from 4°C to 24°C during 10 min resulted in the induction of an uptake process of dextran-FITC (*D*) or BSA-FITC (*H*). (*J*) Distribution histograms of BSA-FITC fluorescence intensity of COS 5-7 cells measured by flow cytometry 1 h after 1-min exposure to LEF of 20 V/cm at 24°C: (*1*) control cells in the absence of BSA-FITC in the medium; (*2*) control cells in the presence of BSA-FITC; (*3*) cells exposed to LEF in the presence of BSA-FITC; and (*4*) same exposed cells as in *3* but further subjected to trypsinization before measurement.

times at 4°C with DMEM-H (210 × *g*; RT6000D, Sorvall) for 5 min and resuspended, usually at 3 × 10^6/ml, in cold (4°C) DMEM-H medium containing different BSA-FITC concentrations (0.1–15 μM). Control and exposed cells were incubated with BSA-FITC for a total period of 5 min at 4°C. Since similar adsorption of BSA-FITC was obtained for 30 min at 4°C, it may be concluded that we reached a steady state. The cells were exposed for 1 min to LEF (20 V/cm, 180 μs, 500 Hz) at 4°C after 4 min of preincubation with the probe at the same temperature. Then the cells were washed three times in cold DMEM-H medium to remove unbound BSA-FITC. Analysis of adsorbed BSA-FITC was carried out by flow cytometry. At 4°C the BSA-FITC binds to the plasma membrane but is not internalized. Nonspecific binding of BSA-FITC was determined by incubating the cells in a 1000-fold excess of unlabeled albumin, with consequent washing. The analysis of the adsorption isotherms was based on a single binding site scheme: $B = (B_{max} \times C)/(K_d + C)$, where C is the probe's concentration, B is the probe adsorption (in terms of G_m), B_{max} is the maximal probe adsorption at high probe concentrations, and K_d indicates the probe-receptor dissociation constant. Curve fitting (of the above expression as well as of Eadie-Hofstee and Hill plots) was performed by the least squares method with Microcal Origin 6 software (Microcal Software, Northampton, MA) using direct weighting to avoid errors at small concentrations.

Uptake by COS 5-7 cells was initiated by suspending the cells in DMEM-H medium containing different concentrations of BSA-FITC. For each uptake assay the probe was in the cells' suspension for a total of 5 min at 4°C (preincubated for 4 min and exposed for 1 min to LEF at 4°C). Then cells were washed once at 4°C and further incubated in the absence of BSA-FITC for an additional 25 min at 24°C. At the end of the incubation cells were treated with 0.01% trypsin for 5 min at 37°C. The efficiency of the removal of BSA-FITC from the cell surface was validated by microscopic visualization. The extent of nonspecific uptake of BSA-FITC was determined by incubating the LEF-exposed and control cells, in a 1000-fold excess of unlabeled albumin, for 15 min at 4°C.

To study the extent of LEF-induced adsorption and uptake of BSA-FITC as a function of time interval after exposure of cells to LEF, the probe was either present during the electric treatment or added to the cell suspension at various times after termination of exposure from zero to 10 min. To differentiate between LEF-induced adsorption and uptake kinetics experiments were performed at 4°C and 24°C.

To determine the dependence of LEF-induced binding and uptake of BSA-FITC on temperature the cells were incubated during and after exposure at different temperatures in the range of 4–37°C, using the same protocols as described above.

Dependence of uptake on electrical parameters and medium composition

The dependence of LEF-induced uptake of BSA-FITC by COS 5-7 cells on the solution's conductance characteristics was studied by performing uptake experiments in solutions of different compositions. DMEM-H medium was mixed with 0.3 M sucrose supplemented with 25 mM HEPES at different proportions (0, 10, 25, 50, 75, and 100%). Cells (3 × 10^6/ml) were resuspended in these solutions in the presence of 6.8 μM BSA-FITC and then exposed to LEF for 1 min at 24°C under different conditions:

1. Varying the conductance of the medium while maintaining a constant electric field strength of 20 V/cm, pulse duration of 180 μs at frequency of 500 Hz.
2. Varying the electric field strength while maintaining a constant current of 140 mA, pulse duration of 180 μs at frequency of 500 Hz.
3. Varying the pulse duration at a constant electric field strength of 20 V/cm and frequency of 500 Hz.

After exposure, the cells were further incubated for 24 min at 24°C. They were washed twice in DMEM-H medium and then subjected to 0.01% trypsin for 5 min at 37°C to remove adsorbed BSA-FITC. LEF-induced uptake of BSA-FITC into COS 5-7 cells was analyzed by flow cytometry. PI (30 μM) was added before analysis to eliminate signals from dead cells.

Adsorption of DNA and DNA-complex to cell membrane after exposure

A 4.7-kb plasmid (GFP S65T, Clontech, Palo Alto, CA) carrying green fluorescent protein was prepared from *Escherichia coli* using Midiprep DNA purification system (Promega, Madison, WI). The plasmid was stochiometrically stained with the DNA intercalating dye PI. The staining was performed with 7.5 × 10^{-5} M dye at DNA concentration of 1 μg/μl for 60 min at 4°C. This concentration yields an average base pair/dye ratio of 4–5 (Golzio et al., 2002). Stained DNA was added to the cell suspension as

a single component or as a complex with either diethylaminoethyl-dextran (DEAE-dextran, 500 kDa), or polyethylenimine (PEI, 2000 Da). The DEAE-dextran-DNA complex was prepared by incubating the labeled DNA plasmid with 1 mg/ml DEAE-dextran for 30 min at 24°C. DNA-PEI complex was prepared by incubating stained DNA with 6 μM of PEI for 30 min at 4°C.

The study of the LEF-induced adsorption of DNA to the cell membrane of COS 5-7 cells was performed by resuspending the cells in DMEM-H medium at 4°C in the presence of PI-labeled plasmid or plasmid complexes. One-half milliliter of cell suspension containing 10^6 cells and 10 μg of labeled plasmid or DNA complex with either DEAE or PEI was exposed to LEF of 20 V/cm for 1 min at 4°C. Due to its high quantum yield the PI-labeled plasmid was used for the quantification of DNA adsorption. Quantitative analysis of DNA binding to cell surface was performed by flow cytometry.

Determination of LEF-induced cell-cell aggregation

To study electric field-induced cell-cell aggregation COS 5-7 cells were suspended in DMEM-H medium at five different cell concentrations: 0.3×10^6; 0.75×10^6, 1.5×10^6, 3×10^6, and 6×10^6 cells/ml. They were exposed for 1 min to LEF of 10 V/cm (pulse duration of 180 μs, 500 Hz). After exposure the 0.5 ml of cell suspension was diluted 100-fold in DMEM-H to minimize spontaneous aggregation.

The time dependence of LEF-induced aggregation was estimated by exposing low concentration of 0.5×10^6 cells/ml to electric stimulation of 10 V/cm (180 μs, 500 Hz) for 1 min. After exposure 0.5 ml of cell suspension was transferred to a large volume (50 ml) of DMEM-H. At different times after exposure in the range of 0–2 h, cells in both control and exposed samples were sedimented down ($210 \times g$ for 3 min) so that they formed a loose pellet of cells, leading to enhancement of cell-cell aggregation. Cell pellets were gently resuspended by a standardized procedure. Detection of cell aggregation was performed using a Coulter counter (Coulter Multisizer, Coulter Electronics, Miami, FL) employing a 100-μm orifice. For each sample, $50–70 \times 10^3$ events were counted and data were collected in a list mode. The extent of LEF-induced cell-cell aggregation was calculated in terms of the percentage of aggregates consisting of two or more cells using the modified procedure of McLean and Hause (1981). First, size distribution parameters were determined for a diluted 0.3×10^6 cells/ml suspension. Then the gating value of single cells' population mean diameter multiplied by 1.2 was chosen for the selection of aggregates.

Statistical analysis

Experiments were conducted at least in triplicate and the mean and standard deviation (SD) were calculated. Significances of differences between groups were assessed by unpaired Student's *t*-test.

RESULTS

Adsorption of BSA-FITC, dextran-FITC, and DNA to cell membrane after exposure to LEF

A 1-min exposure of COS 5-7 cell suspension to a pulsed unipolar train of low electric fields (20 V/cm, 500 Hz, pulse duration 180 μs) at 4°C in the presence of BSA-FITC, dextran-FITC, or DNA in the extracellular medium leads to efficient adsorption of probes to the cell membrane. It is evident that when the exposure was carried out at 4°C the fluorescent probes were essentially confined to the cell membrane in an adsorbed state, with a relatively minor fraction of the probe being in the cell's interior. Horizontal optical sections performed by confocal microscopy (Fig. 1, *C* and *G*) show very efficient LEF-induced adsorption of dextran-FITC and BSA-FITC to the cell membrane, relative to control cell suspension to which the probe was added, but which was not subjected to LEF (Fig. 1, *A* and *E*). Vertical optical sectioning by confocal microscopy (Fig. 1, *B* and *F*) again confirmed the very effective adsorption of dextran-FITC and BSA-FITC to the cell membrane. Furthermore, heating of the cells, which were first exposed to LEF at 4°C, in the presence of the probes, to 24°C during a period of 10 min resulted in the incorporation of the probes into cells. Probes appeared in the cytosol as discrete vesicular structures (Fig. 1, *D* and *H*, for dextran-FITC and BSA-FITC, respectively). These findings demonstrate that the process of incorporation of the fluorescent probes into the cytosol is a temperature-dependent one. The distinction between the fraction of the probe that was adsorbed to the cell surface and the fraction internalized into the cytosol was carried out by effectively removing the BSA-FITC from the cell surface by the proteolytic action of trypsin. Thus, the fluorescence of cells after trypsinization reflects the extent of the probe's uptake by these cells. The exposure of COS 5-7 to LEF of 20 V/cm for 1 min in the presence of 6.8 μM of BSA-FITC at 24°C showed a 10.2-fold rise in BSA-FITC adsorption and 4.5- to 5-fold higher uptake compared to unexposed control cells. HaCaT cells exposed to LEF of 20 V/cm for 1 min in the presence of 6.8 μM of BSA-FITC at 24°C showed a 9.5-fold rise in BSA-FITC adsorption and 6.2-fold higher uptake compared to unexposed control cells. LEF-induced uptake of BSA-FITC into COS 5-7 or HaCaT cells was present in 70–90% of the cell population compared with unexposed ones, in terms of 95% confidence. A similar trend of LEF-enhanced adsorption was found for DNA. Direct microscopic visualization of DNA interaction with plasma membranes of unexposed control COS 5-7 cells at 4°C shows no notable staining (Fig. 2 *A*). However, LEF treatment of COS 5-7 cells in the presence of DNA-DEAE-dextran at 4°C resulted in an appearance of a fluorescence ring at the cell's periphery indicating the adsorption of DNA-DEAE-PI to the cell surface (Fig. 2 *B*). DNA-membrane interaction was not cell-specific and was also observed for a human keratinocyte cell line (HaCaT cells, data not shown).

The comparison of the efficiency of adsorption of different probes to COS 5-7 cells by flow cytometry shows that LEF-induced adsorption of dextran-FITC and BSA-FITC to COS 5-7 cells is 10.0- and 10.2-fold higher, respectively, than in nonexposed samples. Under similar exposure conditions the LEF-induced adsorption of DNA-PI is 1.4-fold higher than in controls. Employing DNA complexes with DEAE-dextran and PEI yielded an LEF-induced adsorption increase of 1.9- and 1.6-fold, respectively.

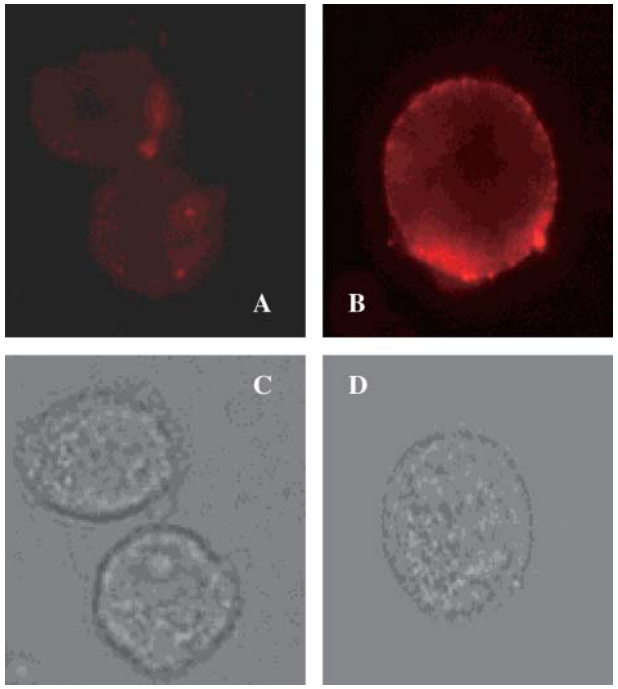

FIGURE 2 Fluorescence microscopy of LEF-induced binding of DNA-DEAE-dextran complex to COS 5-7 cells. Suspension of COS 5-7 cells was incubated with DNA-DEAE-dextran complex at 4°C for 4 min, exposed to LEF of 20 V/cm for 1 min, washed once, then stained with PI and immediately analyzed by fluorescence microscopy. (*A* and *B*) Fluorescence images of control and exposed cells in the presence of DNA complex stained with PI. (*C* and *D*) Complementary Nomarski interference contrast images.

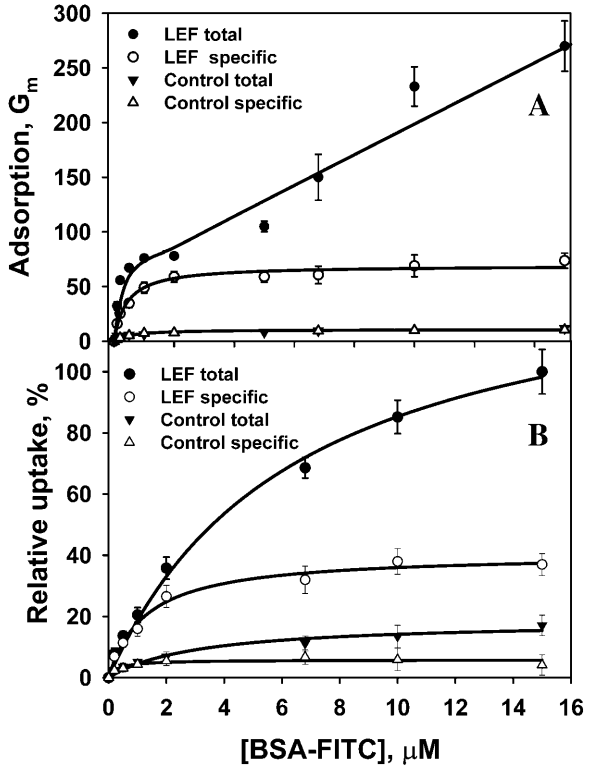

FIGURE 3 Dependence of low electric field-induced adsorption and uptake by COS 5-7 cells on BSA-FITC concentration. (*A*) Low electric field-induced adsorption. Solid circles, total LEF-induced binding; open circles, LEF-induced specific binding; solid triangles, total binding of control cells; open triangles, specific binding of control cells. Cells were suspended in DMEM-H medium containing different BSA-FITC concentrations (0.1–15 μM) at 4°C. The cells were incubated with BSA-FITC for 4 min at 4°C, exposed to LEF (20 V/cm, 180 μs, 500 Hz) for 1 min and washed three times with DMEM solution at 4°C. Nonspecific binding of BSA-FITC was determined by the addition of 1000-fold excess of unlabeled albumin, and the specific binding was calculated. Analysis of adsorbed BSA-FITC was carried out by flow cytometry and presented as the geometric mean (G_m, mean ± SD) of the fluorescence distribution histogram. (*B*) Low electric field-induced uptake. Solid circles, total LEF-induced uptake; open circles, LEF-induced uptake via specific sites; solid triangles, total uptake of control cells; open triangles, specific uptake of control cells. Procedure was the same as in (*A*) where cells were incubated with BSA-FITC at different concentrations in the range of 0.1–15 μM at 4°C, exposed to LEF for 1 min, and washed at 4°C. The cells were further incubated for an additional 25 min at 24°C. At the end of the incubation period the cells were treated with 0.01% trypsin for 5 min at 37°C and determined by flow cytometry. LEF-induced uptake via nonspecific sites was determined by exposing the cells to LEF at 4°C in the presence of different BSA-FITC concentrations. Then the excess of unlabeled BSA was added to the exposed cell suspension at 4°C for 15 min. Consequent procedure involved temperature elevation to 24°C for 25 min, followed by a short trypsinization step and measurement by flow cytometry. The uptake values are given relative to the maximal total uptake and are expressed as mean ± SD. Each data point represents three independent experiments, each in triplicates ($n = 9$), for each probe concentration. Curves are results of fitting (see text).

Dependence of LEF-induced adsorption and uptake on BSA-FITC concentration

The dependence of LEF-induced binding on probe concentration was studied by exposing COS 5-7 cells to LEF in the presence of different concentrations of BSA-FITC in the range of 0–15 μM at 4°C. The total binding of the BSA-FITC probe to the cell surface as well as the nonspecific one (after incubation with 1000-fold excess of unlabeled BSA) were determined by flow cytometry (Fig. 3 *A*). The total binding of BSA-FITC both in LEF-treated and unexposed cells is concentration-dependent. Analyses of the binding data reveal that respective Eadie-Hofstee plots (not shown) for both the constitutive and LEF-induced total binding are curved and may be clearly divided into two linear regions, one with high affinity and low capacity, and another one with low affinity and high capacity. In contrast, the specific binding of BSA-FITC to control and LEF-treated cells is well described as a one-binding site reaction. Taking into account the large differences between high- and low-affinity binding sites, we assume that, in the concentration range studied, the total binding is a sum of specific and nonspecific binding, where the latter linearly increases with concentration. The exact dissociation constants and maximal binding capacities were obtained from nonlinear fitting of the adsorption isotherms (Fig. 3 *A*) as it gives more precise values compared to linear Eadie-Hofstee or Scatchard plots.

The specific binding to both unexposed and LEF-exposed cells was found to saturate at concentrations higher than

$\sim$5 μM. The fitting to one binding site model gives half-maximum saturation concentration of $K^{con}_{D,bind} = 0.51 \pm 0.06$ μM (value $\pm$ fitting error) for unexposed control samples, and $K^{LEF}_{D,bind} = 0.40 \pm 0.05$ μM for the exposed ones. The binding capacity of specific sites on the plasma membrane was significantly (6.5-fold) higher in exposed cells where $B^{LEF}_{max,bind} = 68.9 \pm 1.7$ a.u. as compared to controls, where $B^{con}_{max,bind} = 10.6 \pm 0.1$ a.u.. The specific binding of BSA-FITC to control cells lacks cooperativity (Hill plot slope of 1.07 was not significantly different from 1), while the specific binding of the probe to LEF-treated cells exhibits a weak negative cooperativity with a slope of 0.78 for the Hill plot.

The nonspecific binding of BSA-FITC was found to be linearly dependent on BSA-FITC concentration in the range of 0–15 μM both for control and LEF-treated COS 5-7 cells ($R^2 = 0.78$ and 0.98, respectively). The nonspecific binding of BSA-FITC to control cells is very weak as characterized by a slope S^{con}_{bind} of 0.4 ± 0.09 a.u./μM, while in LEF-treated cells it is $\sim$33-fold steeper, possessing S^{LEF}_{bind} of 13.2 ± 0.6 a.u./μM.

The dependence of LEF-induced uptake on the probe's concentration was examined simultaneously with the binding studies. This was performed by determining LEF-induced internalization into COS 5-7 of different BSA-FITC concentrations in the range of 0.1–15 μM at 24°C. To differentiate uptake via specific binding sites from the total uptake, the cells were incubated at 4°C in the presence of three different BSA-FITC concentrations of 6.8 μM, 10 μM, and 15 μM, and were exposed to LEF, again at 4°C. An excess of unlabeled BSA was then added to exposed and unexposed cell suspensions, and the temperature was raised to 24°C, resulting in an uptake of BSA-FITC only via nonspecific binding sites. The results were analyzed as performed for the binding experiments. The uptake as a function of BSA concentration, normalized to the maximal total uptake, is shown in Fig. 3 *B*. The constitutive process taking place in control cells shows a specific uptake with saturation at concentrations above $\sim$3 μM, possessing apparent $K^{con}_{D,uptake} = 0.30 \pm 0.13$ μM and $B^{con}_{max,uptake} = 9.6 \pm 1.9$ a.u. The nonspecific uptake rises linearly ($R^2 = 0.99$) with BSA-FITC concentration yielding a slope S^{con}_{uptake} of 1.45 $\pm$ 0.05 a.u./μM. The LEF-induced uptake via specific sites reaches saturation at concentrations above $\sim$6 μM. The apparent $K^{LEF}_{D,uptake}$ and $B^{LEF}_{max,uptake}$ for LEF-stimulated specific uptake amount to 1.31 $\pm$ 0.16 μM and 71.2 $\pm$ 3.0 a.u., respectively. The nonspecific LEF-stimulated uptake fits a linear dependence ($R^2 = 0.96$) on BSA-FITC concentration having a slope S^{LEF}_{uptake} of 7.60 $\pm$ 0.51 a.u./μM. The total uptake showed no saturation within the studied concentration range either in exposed or in unexposed cells.

Temperature dependence of electric field-induced adsorption and uptake

Temperature dependence of LEF-induced adsorption (Fig. 4 *B*) and uptake (Fig. 4 *A*) of BSA-FITC (6.8 μM) was investigated by flow cytometry, fluorimetry, and confocal microscopy. We performed LEF-induced internalization of BSA-FITC at different temperatures in the range of 4–37°C. Though the LEF-induced internalization was lowest at 4°C, it could not be completely abolished because of the trypsinization stage, which had to be performed at 37°C. Therefore, the formation of endocytic vesicles was not completely inhibited at 4°C, though further fusion events between vesicles were totally suppressed below 15°C. Thus, BSA-FITC was found to be located in the immediate vicinity of the membrane in both exposed and unexposed cells. However, exposure to LEF at 24°C in the presence of BSA-FITC revealed, by confocal microscopy, the formation of massively patched fluorescent patterns in the cytosol. LEF-induced uptake of

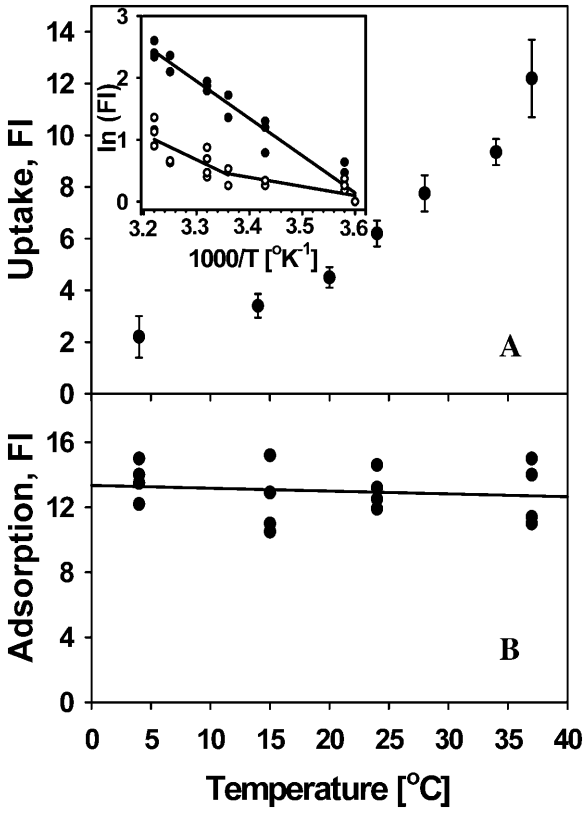

FIGURE 4 Temperature dependence of low electric field-induced uptake (*A*) and adsorption (*B*) of BSA-FITC by COS 5-7 cells. The cells were incubated with BSA-FITC (6.8 μM) in DMEM-H for 4 min and then were exposed for 1 min to LEF at different temperatures (4–37°C). Then cells were washed and incubated for 25 min at the different temperatures, where the adsorption and uptake were determined simultaneously. The LEF-induced uptake is given in terms of FI of G_m relative to its control value. (*Inset*) Arrhenius plots of the total uptake of BSA-FITC: solid circles, LEF-induced uptake; open circles, constitutive uptake. The FI in the Arrhenius plot was relative to the uptake value at 4°C, both for exposed and unexposed samples. LEF-induced adsorption (*B*) was determined by fluorimetric measurement of the BSA-FITC fraction removed from the cell surface after trypsinization. The results are presented as FI relative to unexposed controls. The results are given as mean $\pm$ SD of at least three independent experiments, each in triplicates ($n = 9$).

BSA-FITC was found to be exponentially dependent on temperature (Fig. 4 *A*). The energy of activation, calculated for the constitutive uptake, was 2.9 ± 0.6 kcal/mol ($R^2 = 0.65$) in the temperature range of 4–15°C and 8.1 ± 1.9 kcal/mol ($R^2 = 0.60$) in the temperature range of 15–37°C. However, LEF-induced uptake at all temperatures between 4°C and 37°C was best fitted to a single line reflecting activation energy of 12 ± 0.6 kcal/mole ($R^2 = 0.96$).

The increased uptake is accompanied by a higher amount of vesicular structure in the cytosol, which was detected by fluorescence microscopy. This increase in the formation of intracellular vesicles is also reflected by the LEF-induced rise of the side light scattering from the exposed cells, which was found to be temperature-dependent. The mean level of side scattering, determined by analysis of distribution histograms of flow cytometry experiments, reveals no significant change for untreated cells when increasing the temperature from 4°C to 37°C. Exposure of cells to LEF at 4°C showed no change in side scattering. However, increasing the temperature at which exposure was performed from 4°C to 37°C yielded a monotonous increase of side light scattering reaching a 1.5-fold higher level at 37°C than at 4°C.

In contrast to LEF-induced uptake of BSA-FITC, the LEF-induced adsorption of the probe was found to be independent of temperature. LEF-induced adsorption of the BSA-FITC probe was determined by analyzing the fraction of probe that was removed from the cell surface after the proteolytic action of trypsin. Fig. 4 *B* shows the LEF-induced adsorption determined at 4°C, 15°C, 24°C, and 37°C, compared to control unexposed cells at each temperature. The obtained results demonstrate that there is no statistically significant change in the level of BSA adsorption over the whole temperature range of 4–37°C.

Dependence of adsorption and uptake on time after exposure to LEF

The time course of LEF-induced changes of cell surface leading to increased adsorption of BSA-FITC was examined by adding the probe before exposure or after exposure termination (at different time points in the range of 0–10 min). The study of the temporal adsorption of BSA-FITC to COS 5-7 cells, performed at 4°C (Fig. 5 *A*), shows a maximal 10.2-fold increase of adsorption when the probe was present during LEF treatment. When the probe was added to the exposed cells at different times after exposure, the total binding of the probe to the plasma membrane was only threefold higher than that of controls, a level that was preserved for up to 30 min after the termination of LEF, at 4°C.

Adsorption kinetics of BSA-FITC performed at 24°C (Fig. 5, *B* and *C*) shows again that the most effective adhesion occurs when BSA-FITC is present in the medium during LEF treatment. The maximal adsorption of BSA-FITC was observed when the probe was present in the media during exposure to LEF, showing 10.2 and 9.5-fold increases for COS 5-7 and HaCaT cells, respectively, relative to controls. When the probe was added to cells immediately after the termination of the exposure to LEF, lower values of enhanced binding of 3.2- and 5-fold were obtained for COS 5-7 cells and HaCaT cells, respectively. This enhanced level of adsorption decayed within 10 min after the termination of LEF (Fig. 5 *B*).

The possibility that LEF induces changes in the probe's adsorption characteristics to the cell membrane was examined

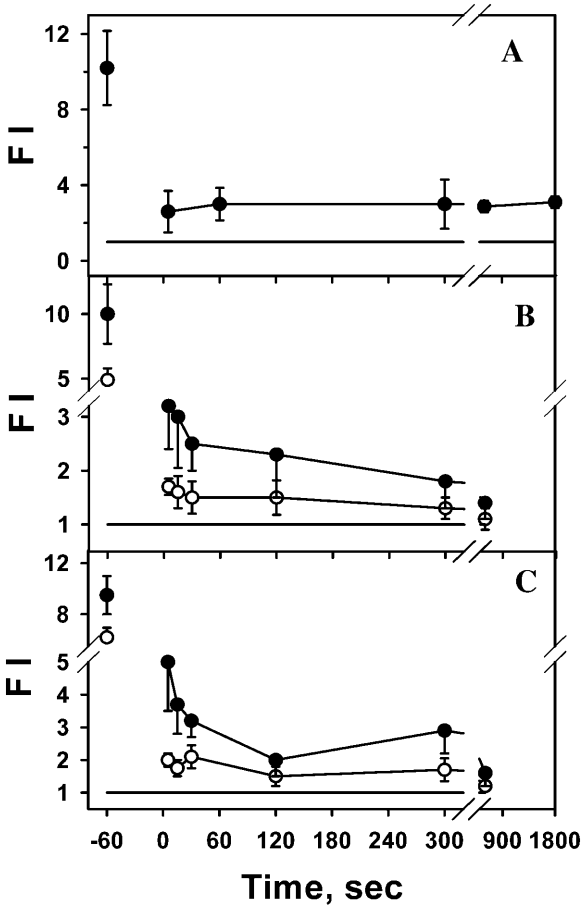

FIGURE 5 Decay kinetics of low electric field-induced adsorption and uptake of BSA-FITC. (*A*) LEF-induced adsorption of BSA-FITC by COS 5-7 at 4°C. (*B*) LEF-induced adsorption (*solid circles*) and uptake (*open circles*) of BSA-FITC by COS 5-7 cells at 24°C. (*C*) LEF-induced adsorption (*solid circles*) and uptake (*open circles*) of BSA-FITC by HaCaT cells at 24°C. The horizontal lines represent the level of control unexposed cells. The zero point on the time axis represents termination of a 60-s exposure to LEF. Each point represents the time at which BSA-FITC was added to the medium after exposure. The data points of −60 s on the *x* axis represent adsorption and uptake of the probe added before the 60-s exposure to LEF. In all cases the presence of the BSA-FITC (6.8 μM) in the medium was limited to 5 min (''pulse labeling''), after which the probe was washed out. Analysis was performed 1 h after exposure by flow cytometry. The data are expressed in terms of FI of G_m relative to unexposed controls. The data points are given as mean ± SD of three independent experiments, each in triplicate ($n = 9$). Standard deviation was omitted when it was smaller than the size of the symbols.

by exposing BSA-FITC only to LEF and then adding it to the cells. The adsorption of exposed BSA-FITC to unexposed cells was negligible and was not different from the adsorption of the unexposed probe to unexposed cells. Small but significant adsorption was detected when the exposed probe was added to exposed cells, yielding adsorption similar to that of the unexposed probe to exposed cells. These findings suggest that LEF-enhanced adsorption changes can be attributed to changes in the cell's surface rather than to conceivable electrochemical modification of the probe.

The decay characteristics of BSA-FITC uptake at 24°C were similar to those of BSA-FITC adsorption. The uptake was maximal when the probe was present during exposure and was 4.9- and 6.2-fold higher for COS 5-7 and HaCaT cells, respectively. Uptake increase of only 1.7- and 2-fold was obtained when BSA-FITC was added to COS 5-7 and HaCaT cells immediately after exposure to LEF. Similar to adsorption, the uptake persisted for up to 10 min after exposure to LEF.

Dependence of adsorption, uptake, and viability on electric field strength

The dependence of adsorption and uptake on electric field strength was examined by exposing cell suspensions of COS 5-7 and HaCaT cells in DMEM-H medium to different electric fields in the range of 2.5–20 V/cm (pulse duration 180 μs, 500 Hz, 1 min total time of exposure), in the presence of 6.8 μM BSA-FITC. Both adsorption and uptake demonstrate a linear dependence of LEF-induced uptake by COS 5-7 cells (Fig. 6 *A*) on electric field strength (correlation coefficients of 0.98 and 0.99 for adsorption and uptake, respectively). Similar results were obtained for HaCaT cells (Fig. 6 *B*). The slopes of the dependence of LEF-induced adsorption on electric field strength relative to that of LEF-induced uptake are 2.2- and 1.5-fold higher for COS 5-7 and HaCaT cells, respectively. The viability of COS 5-7 and HaCaT cells decreased linearly with the electric field in the range of 2.5–20 V/cm (Fig. 6, *C* and *D*). After exposure to the maximal electric field of 20 V/cm, the viability of COS 5-7 and HaCaT cells was 82% and 85%, respectively.

LEF-induced cell-cell aggregation

In addition to increased electric-enhanced adsorption and uptake of the macromolecular solutes we could also observe elevated levels of cell-cell aggregation after exposure to LEF. The increase in cell-cell aggregation after exposure to LEF is visually demonstrated by phase contrast images of control and exposed COS 5-7 cells suspended at a concentration of 3×10^6 cells/ml (Fig. 7, *A* and *B*). Formation of large aggregates consisting of ~20–30 cells can be observed in the exposed cells compared to controls, where

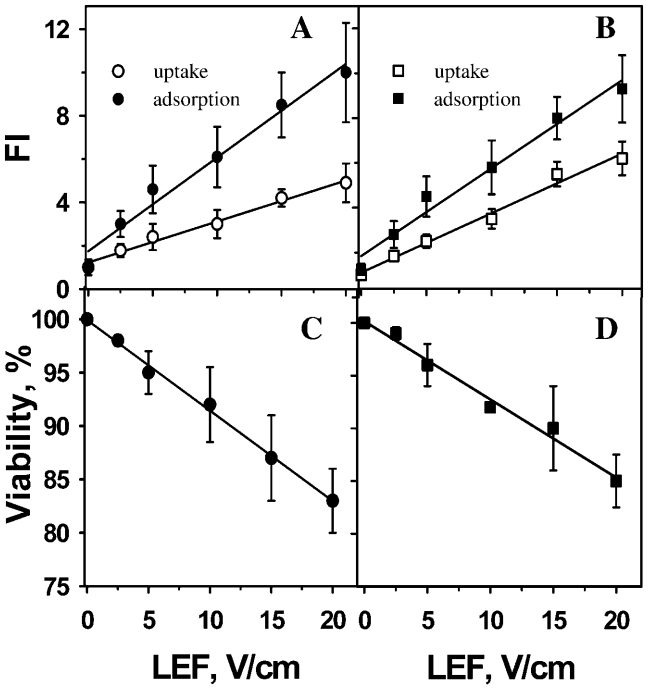

FIGURE 6 Dependence of adsorption and uptake of BSA-FITC and cell viability on electric field strength at 24°C. (*A*) LEF-induced adsorption (*solid circles*) and uptake (*open circles*) by COS 5-7 cells. (*B*) LEF-induced adsorption (*solid squares*) and uptake (*open squares*) by HaCaT cells. (*C* and *D*) Cell viability after exposure to LEF of COS 5-7 (*solid circles*) and HaCaT (*solid squares*) cells, respectively. Exposure was carried out under standard conditions (180 μs pulse width, 500 Hz, total exposure for 1 min). The data of adsorption and uptake are expressed as FI of G_m relative to unexposed cells. The data points are given as the mean ± SD of three independent experiments each in triplicate ($n = 9$). Standard deviation was omitted when it was smaller than the size of the symbols.

spontaneous aggregation occurs to a much lower extent, consisting mostly of two or three cells. The level of aggregation of COS 5-7 cells at different cell concentrations after exposure to LEF of 20 V/cm (frequency of 180 μs, pulse duration of 500 Hz) for 1 min was determined by a Coulter counter (Fig. 7 *C*). When cell concentration in suspension increased, elevated spontaneous formation of cell-cell aggregates took place. Increase of cell concentration from 0.3×10^6 to 3×10^6 in unexposed suspensions resulted in elevation of cell-cell aggregation from 1.5 ± 0.7% to 8.2 ± 4.5%. Exposure of cell suspensions to LEF of 20 V/cm leads to a much larger aggregation at all cell concentrations. Thus, increase in cell concentration from 0.3×10^6 to 3×10^6 resulted in elevation of cell-cell aggregation from 5% to 40% after exposure. At the higher concentration of 6×10^6 cells/ml 60% of cells appeared as aggregates. It should be stressed that due to the limit of the 100-μm orifice used in the Coulter counter instrument, large cell aggregates could not be measured. Thus our data represent a low estimation of the extent of LEF-induced aggregation.

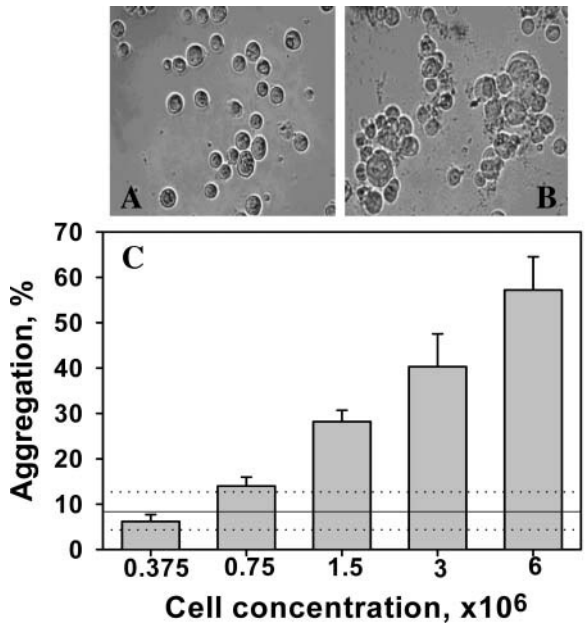

FIGURE 7 Low electric field-induced cell-cell aggregation. COS 5-7 cells suspended in DMEM-H medium at different cell concentrations in the range of 0.3–6 $\times$ 10^6/ml, were exposed for 1 min to LEF (20 V/cm, 500 Hz, 180 μs). After exposure, the cells were diluted by 100-fold in DMEM-H without further washing, and analyzed both by phase contrast microscopy and Coulter counter. (*A* and *B*) Phase contrast images of control and exposed cells (3 $\times$ 10^6/ml), respectively. (*C*) Dependence of LEF-induced cell-cell aggregation on cell concentration. The horizontal line represents the level of spontaneous aggregation of control unexposed cells (at a concentration in the range of 0.5–3.0 $\times$ 10^6/ml). Each data point, expressed as mean $\pm$ SD, represents three independent experiments ($n = 6$).

Kinetics of cell-cell aggregation

To evaluate the temporal characteristics of the cellular changes leading to the observed increase of cell-cell aggregation we measured the level of aggregation at different times after exposure (Fig. 8). COS 5-7 suspensions of 0.5 $\times$ 10^6 cells/ml (which yields very low spontaneous aggregation) were exposed to LEF of 20 V/cm for 1 min at 24°C. After exposure cells were brought into close contact by centrifuging them at different times in the range of 0–2 h. The formed cell pellet was resuspended by weak standard stirring and consequently analyzed by a Coulter counter. LEF-induced formation of aggregates was compared with controls which were either nontreated but centrifuged cells (20 $\pm$ 2%) or cells exposed to LEF but not centrifuged (22 $\pm$ 5%). The maximal LEF-induced aggregation of ~33% is maintained provided the cells are brought into contact by centrifugation within 20 min after exposure. However, 30 min after exposure the ability of cells to form aggregates decreases to that of exposed but not centrifuged cells. The extent of cell-cell aggregation 60 and 120 min after exposure does not differ from controls. These findings suggest that LEF induces a long-lasting modification of cell surface which contributes to the increased ''sticky'' character of the cells toward each other.

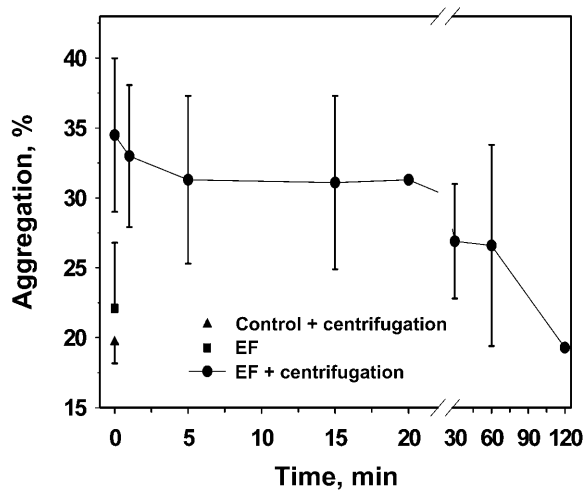

FIGURE 8 Decay kinetics of low electric field-induced cell-cell aggregation. COS 5-7 cells at concentration of 0.5 $\times$ 10^6/ml were exposed to LEF for 1 min. At different times after exposure, the cells were sedimented by centrifugation to increase cell-cell aggregation both in control (*solid triangle*) and exposed samples (*solid circles*). The exposed, but non-centrifuged cells are designated by a solid square. Analysis of cell-cell aggregation was performed by Coulter counter. Each data point, expressed as mean $\pm$ SD, represents three independent experiments ($n = 6$).

Effect of medium conductivity on LEF-induced BSA-FITC uptake

To assess the dependence of LEF-induced uptake of BSA-FITC on medium conductivity, we performed uptake studies using solutions of different composition. DMEM-H medium was diluted at different ratios with 0.3 M sucrose supplemented with 25 mM Hepes. COS 5-7 cells were suspended in these solutions, possessing different conductivities, in the presence of 6.8 μM of BSA-FITC, and then exposed to LEF for 1 min at 24°C, maintaining constant electric parameters of electric field strength of 20 V/cm, pulse duration of 180 μs, and frequency of 500 Hz. It is evident from Fig. 9 *A* that increasing medium conductivity from 6.4 to 18.6 mS/cm resulted in a corresponding increased uptake of BSA-FITC into cells by up to 8.8-fold. The dependence of the uptake on medium conductivity fits best to a quadratic dependence (coefficient of determination of 0.99 as compared with a lower value of 0.95 for linear regression). The viability of COS 5-7 cells exposed to LEF declined linearly down to 80% with increased conductance (Fig. 9 *D*).

Effect of electric field strength on BSA-FITC uptake under constant current

To study the dependence of LEF-induced uptake of BSA-FITC on LEF strength, we performed exposure experiments in solutions of different composition in the presence of 6.8 μM BSA-FITC. The cells were exposed, at 24°C, to LEF of different intensities, 0–43 V/cm, under conditions of constant current of 140 mA, frequency of 500 Hz, pulse

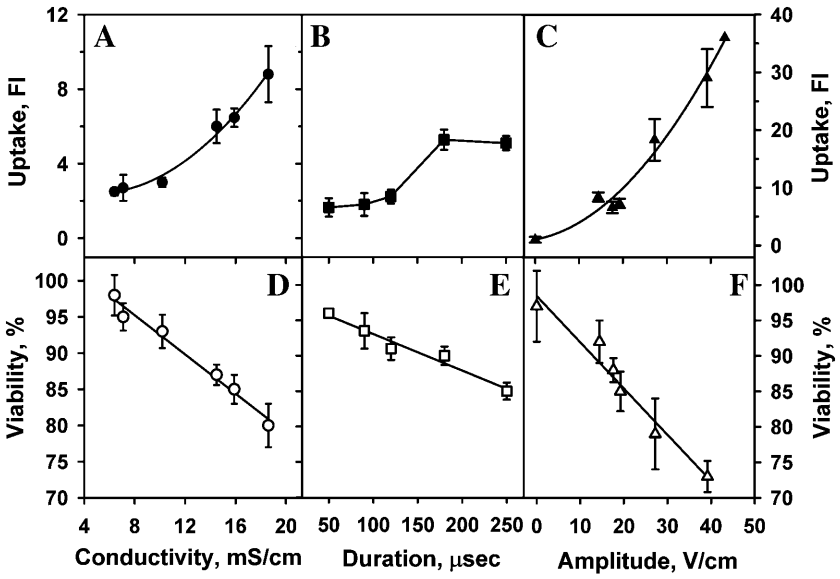

FIGURE 9 Dependence of BSA-FITC uptake and viability of COS 5-7 cells on the electrical parameters. (*A*) Effect of medium conductivity on LEF-induced BSA-FITC uptake under constant electric field strength of 20 V/cm (pulse duration 200 μs, 500 Hz). Conductance changes were produced by suspending COS 5-7 in isotonic mixtures of DMEM with 0.3 M sucrose (DMEM, DMEM 10% v/v sucrose, DMEM 25% sucrose, DMEM 50% sucrose, DMEM 75% sucrose, 100% sucrose) in the presence of 25 mM HEPES and 6.8 μM BSA-FITC. (*B*) Dependence of BSA-FITC uptake on pulse duration (in the range of 50–250 μs) under standard conditions maintaining constant electric field of 20 V/cm (500 Hz, 1 min total exposure) and constant medium conductance (DMEM-H). (*C*) Dependence of BSA-FITC uptake on the amplitude of the electric field, in the range of 0–43 V/cm, under a constant current (140 mA). All cell suspensions (1.5×10^6 cells/0.5 ml) were exposed for 1 min to the different electric field parameters in the presence of 6.8 μM of BSA-FITC. (*D–F*) Viability of COS 5-7 cells after exposure to electric field parameters shown in *A–C*, respectively. Each data point, expressed as mean ± SD, represents three independent flow cytometric experiments, each in duplicate ($n = 6$).

duration of 180 μs, and total time of exposure of 1 min. As shown in Fig. 9 *C*, uptake increases with the rise in electric field strength. Exposure at 43 V/cm leads to a 36-fold increase of BSA-FITC uptake. The dependence of the uptake on electric field strength best fits a quadratic dependence (coefficient of determination of 0.98, as compared with a lower value of 0.92 for a linear regression). At the same time cell viability decreased down to 73% when increasing electric field strength to 43 V/cm (in sucrose 0.3 M + Hepes 25 mM, isotonic medium) (Fig. 9 *F*).

Effect of pulse duration on BSA-FITC uptake

The dependence of LEF-induced uptake of BSA-FITC on pulse duration was studied by exposing COS 5-7 cells in DMEM-H medium for 1 min at 24°C while keeping all other parameters constant (electric field strength of 20 V/cm, current of 140 mA, frequency of 500 Hz). Increasing pulse duration from 50 to 250 μs resulted in a corresponding increase in the uptake of BSA-FITC into cells by up to fivefold (Fig. 9 *B*). The LEF-induced uptake showed a sigmoidal dependence on pulse duration (Fig. 9 *F*). Viability of COS 5-7 cells exposed to LEF of 20 V/cm decreased linearly down to 85% upon lengthening pulse duration up to 250 μs.

DISCUSSION

Stimulation of adsorption by low electric fields

Possible mechanisms underlying the enhancement of adsorption

Exposure of cells to a low unipolar electric field may lead to at least two distinct primary effects at the level of the cell membrane: 1), electric polarization of the membrane, leading to alteration of the transmembrane potential (Schwan, 1957); and 2), in situ ''lateral electrophoresis'' of charged proteins and lipids in the plane of the cell membrane (Poo, 1981).

The exposure of a cell to external electric field leads to the induction of a transmembrane polarization ($\Delta\psi$) given by (Schwan, 1957, Farkas et al., 1984)

$$\Delta\psi_\theta = 1.5 \times E_{ex} \times r \times \cos\theta, \quad (1)$$

where E_{ex} is the external electric field, r is the spherical cell radius and θ is the angle between the radius vector to any point in the plasma membrane and the vector of the electric field. Thus, exposure of a cell possessing radius of $\approx$8 μm to the electric field in a range of 2.5–20 V/cm (used in our studies when employing highly conductive media) will result in an induced potential difference 3–24 mV across the plasma membrane. Therefore, the membrane region facing the anode will be hyperpolarized by 3–24 mV; that facing the cathode will be depolarized to the same extent. Though these changes in the transmembrane potential do not lead to electroporation (Rosemberg and Korenstein, 1997; Antov et al., 2004), the possible involvement of the induced transmembrane potential in the uptake process cannot be ruled out. It may alter ion fluxes across the membrane, either through modulation of ion channels or via electric field-induced conformational changes of transport systems. The latter has been suggested by numerous studies that formulated an electroconformational coupling model (Chen and Tsong, 1994, Xie et al., 1997, Tsong, 2002, Tsong and Chang, 2003). The model implies that low electric fields can drive oscillations or fluctuations of enzyme conformation between two states. However, since changes in trans-

membrane potential difference have not been previously reported to directly cause cell surface alterations, they cannot explain the observed LEF-induced enhancement of BSA binding to the cell surface, which occurs even at low temperatures, or the measured increase in cell aggregation.

The other possible primary effect induced in cells exposed to low electric fields is that of electrophoretic induced segregation of labile charged lipids and proteins in the plane of the cell membrane (Fig. 10). This phenomenon was previously explored both theoretically and experimentally (e.g., Jaffe, 1977; Poo and Robinson, 1977; Poo et al., 1979; Poo, 1981; McLaughlin and Poo, 1981; Sowers and Hackenbrock, 1981). It has been pointed out that the external electric field tangential to the cell surface (E_θ) is the driving force (Eq. 2):

$$E_\theta = 1.5 \times E_{ex} \times \sin\theta, \quad (2)$$

where E_θ will induce electrophoretic mobility toward the anodic or cathodic sides of the cell, either by direct electrophoretic mobility of the negatively charged components or by electroosmosis, respectively (McLaughlin and Poo, 1981). Though most studies of lateral electrophoretic segregation of charged membrane components have been carried out on adherent cells employing low DC electric fields (e.g., Poo, 1981; Wang et al., 2003), it was shown that a similar segregation phenomenon could be induced in photosynthetic membrane vesicles of a size comparable to that of cells (Brumfeld et al., 1989; Miller et al., 1994), when exposed in suspension to a train of unipolar pulsed electric fields of duration much shorter than the rotational time of the vesicles. Under these conditions the membrane vesicle can be considered to be in a rotational stationary state, at which time the lateral electrophoretic displacement takes place. Similarly, taking into account that the mean average radius of a COS 5-7 cell is ~8 μm, its rotational time constant, according to the Stocks-Einstein equation, is ~7.5 min. Thus, the exposure to LEF in all our experiments was restricted to 1 min so that it would be much shorter than the rotational diffusion relaxation time of the cell. The short exposure time to LEF is another feature that sets our study apart from previous ones. Exposure to DC electric field of 10 V/cm for 45 min to 3 h was shown to induce asymmetric distribution of acetylcholine receptors in embryonic muscle cells (Orida and Poo, 1978). Similar exposure to DC electric fields of 10 V/cm applied for 30 min induced asymmetry in the distribution of Con A receptors in *Xenopus* muscle cells (McLaughlin and Poo, 1981). In addition, cathode-directed accumulation of epidermal growth factor receptors in corneal epithelial cells was shown to occur after exposure to 3 V/cm for 20 min, whereas similar accumulation of fibroblast and transforming growth factor receptors occurred when exposed to a DC electric field of 1.5 V/cm for 12 h (Zhao et al., 1999). It emerges from these studies that global segregation of membrane receptors, reflected by their asymmetric distribution between the cell hemispheres facing the cathode's or anode's sides, occurs only after relatively long exposure time. Therefore, in the case of a brief exposure we may expect the induction of limited short-range electrophoretic mobility leading to localized segregation of membrane proteins and lipids. It can be proposed that the formation of small receptor aggregates formed after short exposures is reversible differing from the irreversible formation of large aggregates created by prolonged exposure to electric fields (Poo, 1981). This proposal is in agreement with our finding of the transient ability of the cells to form aggregates after LEF termination.

The tangential electric field acts on both charged lipids and proteins (e.g., glycolipids and glycoproteins), leading to the segregation of these membrane components, accompanied by changes in the local charge density (Fig. 10 *b*). Thus it is expected that the cells' areas, depleted of negative charges, will, upon cell-cell collision, be more effective in forming attachment compared to the situation where a higher density of negative charges is present in the area of the two colliding

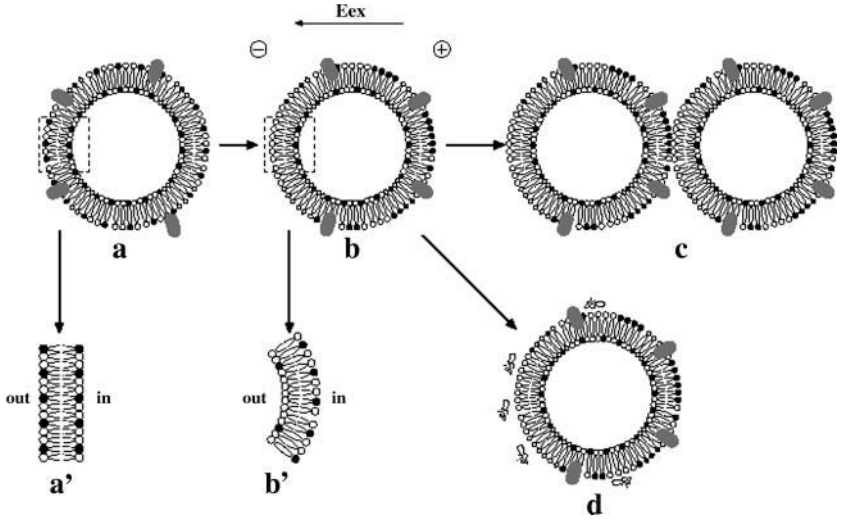

FIGURE 10 Scheme of the suggested mechanism underlying LEF stimulation of adsorption and uptake processes. (*a*) Evenly distributed charged membrane components—lipids (*black circles*) and proteins (*shaded ovals*)—in the plasma membrane of an unexposed cell. (*b*) Segregation of charged membrane components in the outer lipid leaflet of the plasma membrane after short exposure to pulsed low electric fields. (*a′* and *b′*) Spontaneous curvature of the plasma membrane before and after exposure to LEF. These changes are attributed to alteration of LEF-induced charge density in the outer leaflet of the plasma membrane, resulting in a difference between surface charge densities of the two leaflets. (*c*) Aggregation of two cells after electrophoretically driven segregation of charged membrane components in the outer monolayer of the plasma membrane. (*d*) Enhanced adsorption of macromolecules to the plasma membrane at areas depleted of charged membrane components.

cell surfaces (Fig. 10 *c*). Moreover, the existence of segregated areas may favor the increased adsorption of different macromolecules to the cell surface (Fig. 10 *d*).

LEF stimulates adsorption of macromolecules to the cell surface

This study demonstrates that a short exposure to LEF leads to electric field-driven enhancement of adsorption of macromolecular solutes of different chemical nature to the cell membrane. Employment of three different types of macromolecules, BSA-FITC (66 kDa), dextran-FITC (2000 kDa), and DNA (4.7 kb; 3102 kDa) leads to their LEF-enhanced adsorption to the cell surface. Though BSA-FITC and dextran-FITC possess different molecular weights, dissimilar negative charges (~42 and ~222, respectively, per molecule at pH 7.4), various shapes, and different hydrophilic/hydrophobic characteristics, they show comparable LEF-induced adsorption to the cell surface of 10- and 10.2-fold higher, respectively, than that in controls. However, the LEF-stimulated adsorption of the negative fluorescent DNA-PI complex or its positive tertiary complexes DNA-PI-DEAE and DNA-PI-PEI is only 1.4, 1.9, and 1.6-fold higher, respectively, than that of controls. This lower adsorption of DNA as compared with that of dextran of a similar molecular weight may be attributed to the higher surface charge density of DNA and its lower flexibility. These findings suggest that LEF-enhanced adsorption to the cell surface is a characteristic common to different macromolecules. Furthermore, the adsorption of a molecule to the cell surface is determined by many different variables, such as electrostatic and Van der Waals forces, hydrophobicity, molecular geometry of the interacting molecule, the heterogeneous character of the cell surface, and the existence of specific binding sites. Thus, due to the complexity of this system it is not yet possible to quantitatively discuss the relationship between molecular characteristics and the extent of LEF-induced adsorption to the cell surface of a target macromolecule.

The enhancement of adsorption by LEF can be ascribed to two main processes. The first one is the LEF-induced increase in the velocity and rate of collision between the macromolecular solutes and cells. The second process is the LEF-induced alteration of the cell surface, probably through electrophoretic lateral segregation of membrane components. Discrimination between these two processes emerges from examining the kinetic patterns of BSA adsorption to the cell surface (Fig. 5). A threefold higher adsorption is obtained when BSA is added to cells before their exposure to LEF as compared to BSA addition immediately after the termination of exposure. This increase may be attributed to the difference between the electrophoretic mobilities of cells and macromolecular solutes as well as to their accumulation near the anode, which is expected to increase the collision rate between them during exposure, thereby leading to a higher extent of adsorption. At the same time LEF induces changes in the cell membrane, resulting in a cell surface more sticky toward macromolecules. Although elevated collision rate takes place only during LEF treatment, cell surface alteration also persists after LEF termination. Thus, comparing the adsorption levels in the presence and absence of electrophoretic forces (when BSA is added before or after exposure, respectively) allows us to roughly estimate that ~70% of the increase in the total adsorption is attributed to the electrophoretically enhanced collision rate between the altered surface of the cells and the solute macromolecules. The remaining 30% of the total adsorption is attributed to a diffusion rate-limited adsorption of the macromolecules to the electrically modified surface of the cells.

The stimulation of cell surface alteration by LEF seems to be temperature-independent as reflected by similar levels of induced adsorption of BSA-FITC at 4°C and 24°C immediately after the termination of exposure (compare Fig. 5, *A* and *B*). This finding is in agreement with the weak dependence (Q_{10} of 1.2) of membrane receptor segregation by DC electric fields on temperature (Poo, 1981). However, reversibility of the LEF-induced surface alterations is temperature-dependent. The LEF-induced elevated adsorption of BSA-FITC decays to half maximal value within 2 min at 24°C, whereas at 4°C it is maintained for at least 30 min (Fig. 5). Thus it should be pointed out that the LEF-enhanced adsorption taking place at 4°C can be considered to occur under equilibrium conditions, whereas that occurring at elevated temperatures is dominated by kinetic aspects.

Additional evidence for the LEF-induced alteration of the cell membrane stems from the observation of cell-cell aggregation. (Figs. 7 and 8). This aggregation takes place both in the absence and presence of macromolecular probes in the external medium, suggesting that the cell membranes themselves, and not the probes, are primarily modified by LEF. Thus, the dependence of LEF-induced cell-cell aggregation on cell density originates from both enhanced adsorptive properties of the cell surface and the diffusion-limited collision rate. Naturally, if the cell population possesses heterogeneous values of electrophoretic mobilities, an additional electrophoretic contribution to cell aggregation is expected to be proportional to the width of the distribution histogram of the electrophoretic mobilities. Moreover, cells treated by LEF in dilute suspensions ($\sim 5 \times 10^5$ cells/ml), when brought in close contact by centrifugation, preserve their ability to form aggregates for up to 15–20 min after the exposure, at 24°C. However, with time the level of cell aggregation diminishes. The LEF induction of cell-cell aggregation decays to its half-maximal value within 30 min at 24°C, demonstrating again that the LEF-induced surface modification is a reversible one.

Electric field-induced changes, leading to increased adsorption properties of the cell surface, have been previously reported when employing very high electric fields. The exposure of suspension of cells and large unilamellar vesicles to high short electric pulse (100 μs of 3–4 kV/cm)

led to increased cell-liposome adhesion (Chernomordik et al., 1991). This electric field-induced higher affinity for liposomes was found to possess a lifetime of several minutes, similar to the LEF-induced adsorption changes, suggesting that both LEF and high electric fields may share a common feature in modifying the cell surface.

LEF enhances specific and nonspecific adsorption of BSA to the cell surface

More insight into the LEF-driven adsorption of macromolecules to cells was gained by an extended study of the characteristics of LEF-enhanced adsorption of BSA to COS 5-7 cells. Analysis of the adsorption isotherms of BSA-FITC to the surface of COS cells at 4°C, assuming they occur at equilibrium, shows that the total adsorption is characterized by specific and nonspecific binding in both cells subjected to LEF and in unexposed control cells. The specific adsorption may be described by a classical one-binding site model with saturation at BSA concentration ≥ 5 μM. The nonspecific binding fits a linear rise with concentration. The affinity of specific binding does not change significantly after exposure to LEF possessing $K_{\mathrm{D,bind}}^{\mathrm{con}} = 0.51 \pm 0.06$ and $K_{\mathrm{D,bind}}^{\mathrm{LEF}} = 0.40 \pm 0.05\,\mu$M before and after exposure, respectively. However, the number of specific binding sites ($B_{\mathrm{max,bind}}$) increases dramatically by 6.5-fold after LEF treatment. We can speculate as to the identity of the specific binding sites for BSA in COS 5-7 cells by considering the characteristic albumin receptors that exist in similar cells. Taking into account the kidney origin of the COS 5-7 cell line, these receptors could possibly be identified as cubilin and megalin (Christensen and Birn, 2002), though the presence of other receptor types such as gp60, gp31, and gp18 cannot be excluded (Tiruppathi et al., 1997; Schnitzer and Bravo, 1993). The reported K_{d} of these receptors for albumin is in the range of 0.3–0.6 μM (Gekle et al., 1996; Birn et al., 2000;Yammani et al., 2002), which is in good agreement with the value of 0.51 μM obtained for unexposed COS 5-7 cells. The absence of significant changes in the K_{d} values after exposure to LEF suggests that membrane receptors do not undergo LEF-induced substantial structural change sufficient to alter their affinities. However, the significant elevation of the capacity of the cell surface for specific binding after exposure suggests that LEF treatment of cells leads to exposure of binding sites on the cell surface that were unavailable for binding before the LEF treatment. The possibility that exposure to LEF brings about the incorporation of additional receptors from the cytoplasm (LEF-stimulated exocytosis) can be discarded, since it is not plausible for this process to take place at 4°C. An attractive explanation may be put forward in view of recent findings showing strong changes in local dipole potential at the cell membrane interface due to human serum albumin binding (O'Shea, 2003). Treatment of cells with cholesterol or 6-ketocholestanol was shown to lead to increased membrane dipole potential and augmentation of binding reaction with albumin via higher binding capacity without major changes in the affinity (Asawakarn et al., 2001; O'Shea, 2003). Since the employed LEF is sufficient to alter the local dipole potential at the membrane-water interface, it may cause an increase in the number of receptors available for BSA binding. Another possible explanation may be attributed to segregation of charged lipids and membrane proteins along the cell surface taking place upon exposure to electric fields (Jaffe, 1977; Poo, 1981). This notion is in agreement with the findings that cationized ferritin substantially increases binding of albumin to cultured aortic smooth muscle cells (Sprague et al., 1985). The effect was attributed to cationized ferritin-triggered segregation of surface anionic sites resulting in intervening areas essentially devoid of negative charge, thus reducing the electrostatic repulsion between negatively charged human serum albumin and cell surface. Since the possible segregation of plasma membrane receptors is a nonselective process we would like to speculate that the observed phenomena is a general one, not confined to BSA receptors only.

The nonspecific binding of BSA-FITC is also dramatically altered by LEF. The nonspecific components of binding for both control and exposed samples seem to rise linearly with BSA-FITC concentration. However, the slope of the LEF-induced nonspecific binding is 33-fold higher than that of control. It may be proposed that this low affinity and high capacity of BSA binding to the cell surface is associated with hydrophobic interactions of lipids in the outer leaflet of the plasma membrane with albumin molecules. There are 11 hydrophobic pockets known in human serum albumin that are responsible for the binding of fatty acids (Hamilton, 2002). Albumin was reported to preferentially adsorb onto hydrophobic surfaces (Ying et al., 2003; Martins et al., 2003) and to neutral liposomes (Yokoyama et al., 2002). It may be argued that decreased repulsion and increased binding between BSA and the cell surface will be attained when the negatively charged molecular components, exposed to the extracellular milieu, are unevenly distributed along the cell surface due to lateral electrophoresis in the membrane plane. Electric fields of 10–30 V/cm, similar to the ones used in this study, were shown to induce lipid segregation when applied tangentially to a supported bilayer consisting of charged and uncharged lipids (Groves et al., 1997). The measured velocity of charged lipids in the supported lipid bilayer was 6 μm/min (Groves et al., 1998), which is comparable to a mean radius of ~ 8 μm for cells used in our study. External inhomogeneous electric fields applied to cholesterol-phospholipid monolayers were shown to lead to phase separations under appropriate conditions (Radhakrishnan and McConnell, 2000). Thus, LEF-induced segregation between charged and uncharged components on the cell surface is expected to increase nonspecific BSA binding to lipid areas depleted of the anionic charged components.

Low electric fields enhance uptake

On the relationship between LEF-induced adsorption and uptake

The stimulation of uptake via adsorptive endocytic pathway(s) requires, at the first stage, enhanced adsorption to the cell surface. To be able to differentiate between LEF-stimulated processes of adsorption and uptake we made use of the finding that whereas adsorption is independent of temperature, uptake is a temperature-dependent process. We demonstrate that LEF-enhanced adsorption carried out at 4°C is consequently followed by enhanced uptake upon increasing the temperature to 24°C (Fig. 1, *A–H*), suggesting that the two processes are consecutive. Furthermore, the association of these two processes is compatible with the finding that both processes decay at similar rates at 24°C (Fig. 5, *B* and *C*). These similar kinetics do not depend on the cell type and were demonstrated to occur in both cell lines used. Moreover, both LEF-stimulated adsorption and uptake show linear dependence on electric field strength in the range of 2.5–20 V/cm, where the uptake is less steep than the adsorption. The fact that the level of LEF-enhanced uptake is always lower than that of adsorption probably reflects the fact that not all sites on the plasma membrane that are occupied by adsorbed macromolecules can undergo internalization.

The dependence of uptake on temperature emerges from Arrhenius plots of constitutive and LEF-induced uptake processes. Arrhenius plot of constitutive uptake reveals the existence of a biphasic dependence on temperature possessing activation energies of 3 and 8 Kcal/mole for the lower and higher temperature regions, respectively. The presence of biphasic Arrhenius plots in fluid-phase endocytosis was correlated with lipid-phase transition in two renal epithelial cell lines at a similar temperature range (Mamdouh et al., 1996). In contrast, the LEF-induced uptake is best characterized by single activation energy of 12 Kcal/mole. If one perceives electroendocytosis as a process that stimulates the rate of constitutive endocytosis, one would expect it to lead to lower activation energy than that of the constitutive processes. The higher activation energy for the LEF-induced process suggests that the rate-limiting step in the process is probably not the step shared by both LEF and constitutive endocytosis, but rather a step involved in initiating the LEF-induced process. The comparison of efficiency of BSA uptake when exposure is done at 4°C followed by elevating the temperature to 24°C with that of a direct exposure at 24°C shows a much higher uptake for the latter case. Taking into account that the extent of adsorption is temperature-independent, this difference in uptake may be attributed to the fact that the rate of a temporal temperature-dependent stage in the LEF-induced uptake is higher at elevated temperatures.

To determine whether specific or nonspecific binding sites of BSA undergo preferred internalization we studied the uptake process over the same concentration range of BSA that was employed for adsorption studies (Fig. 3 *B*). Comparison of adsorption and uptake isotherms for constitutive processes sheds light on several features.

Specific adsorption and uptake show very similar dependence on BSA concentration, i.e., $K^{con}_{D,bind} = 0.51 \pm 0.06$ and apparent $K^{con}_{D,uptake} = 0.30 \pm 0.13$ μM and $B^{con}_{max,bind} = 10.6 \pm 0.1$ a.u. and $B^{con}_{max,uptake} = 9.6 \pm 1.9$ a.u., respectively (the differences are statistically insignificant).

1. The efficiency of constitutive uptake via specific binding sites (receptors) is very close to 100% over the whole concentration range studied, i.e., throughout the period of 30 min in which the uptake process is measured, almost all BSA bound to specific sites undergoes internalization.
2. Nonspecific constitutive uptake of BSA occurs mostly through fluid-phase endocytosis since its dependence on concentration is steeper than that of adsorption ($S^{con}_{uptake} = 1.45 \pm 0.05$ versus $S^{con}_{bind} = 0.4 \pm 0.09$ a.u./μM, $p < 0.001$).

   The features of constitutive specific BSA uptake fit a binding-limited one-step internalization model (Wiley, 1988; Lund et al., 1990).

For the LEF-stimulated uptake processes the findings are different.

1. Internalization via specific sites is less effective than binding at low BSA concentrations ($K^{LEF}_{D,uptake} = 1.31 \pm 0.16$ μM for uptake and $K^{LEF}_{D,bind} = 0.40 \pm 0.05$ μM for binding, $p < 0.005$), though at higher BSA concentrations all bound BSA molecules are internalized (B^{LEF}_{max} for uptake and adsorption do not differ). This outcome is in agreement with the view that high levels of occupied surface receptors effectively saturate the endocytic apparatus (e.g., limited by amount of adaptor proteins) (Wiley, 1988; Lund et al., 1990).
2. LEF-stimulated uptake via nonspecific sites ($S^{LEF}_{uptake} = 7.60 \pm 0.51$ a.u./μM) corresponds to internalization of more than half of the nonspecifically bound BSA ($S^{LEF}_{bind} = 13.2 \pm 0.6$ a.u./μM).

Analysis of the uptake process as a function of concentration (Fig. 3 *B*) illustrates that, for example, at 6.8 μM BSA LEF-induced specific endocytic pathway constitutes ~50% of the total uptake. Taking into account our previous finding that ~25% of the total LEF-induced BSA uptake is suppressed by inhibitors of clathrin-dependent endocytosis (Antov et al., 2004), it can be suggested that clathrin-mediated uptake is responsible for half of the LEF-induced specific uptake. The other half of the specific LEF-induced BSA incorporation may occur via receptors associated with clathrin-independent pathways.

It should be noted that the observed 5.9-fold higher total uptake after exposure to LEF may originate from the enhanced adsorption of BSA to the cell membrane and from accelerated internalization. A support for the notion of LEF-induced

stimulation of endocytic rate emerges from the observation of the rise in side light scattering after exposure to LEF. This was attributed to the formation of elevated amounts of vesicular structures in the cytosol after exposure to LEF, which was also validated microscopically (Antov et al., 2004). Moreover, the report that LEF stimulates the uptake of fluid phase (Antov et al., 2004) again supports the notion of LEF-induced enhancement of the rate of cell membrane internalization. Thus it may be concluded that exposure of cells to LEF induces increased uptake through augmented adsorption to the cell membrane as well as through an enhanced rate of internalization.

Possible mechanism for enhancement of uptake by low electric fields

The experimental findings imply that LEF-induced cell surface changes and uptake occur by a sequential mechanism. Thus, we suggest that electrophoretic segregation of charged components at the cell surface is also responsible for the stimulated uptake via changes in the membrane's elastic properties. This occurs due to the fact that the tangential electric field acts only on molecules that are associated with the external lipid leaflet of the cell membrane. This is expected to induce segregation of both charged lipids and peripheral proteins that are anchored to the external leaflet, whereas those associated with the inner leaflet will remain unaffected (Fig. 10 *b*). This will lead to changes in the ratio between surface charge densities of the outer and the inner leaflets of the plasma membrane.

Formation of an endocytic vesicle involves bending of the plasma membrane toward the cytoplasm, formation of a membrane bud connected to the plasma membrane by a narrow neck, and, finally, fission of the neck and separation of the vesicle from the mother membrane. Hence, the whole process depends on the tendency of the membrane to bend toward the inside of the cell and to undergo fission. The membrane elastic properties, determining the two tendencies, are the spontaneous curvature, J_S, and the Gaussian modulus (saddle-splay modulus), $\bar{\kappa}$ (Helfrich, 1973). We show below that the LEF-induced segregation of membrane components may result in endocytosis promoting local changes of both the spontaneous curvature and the Gaussian modulus.

Conventionally, the spontaneous curvature is defined as positive if it corresponds to a tendency of the membrane to bulge toward the outside of the cell. Therefore, for stimulation of endocytosis, the membrane spontaneous curvature has to become locally negative, $J_S < 0$. The membrane spontaneous curvature can be expressed through the membrane curvatures of its monolayers,

$$J_S = \frac{1}{2} \times \left(J_S^{out} - J_S^{in}\right), \tag{3}$$

where the superscripts ''out'' and ''in'' correspond to the outer and inner monolayers, respectively. The spontaneous curvature of each monolayer depends on the absolute value of the electric charge density, σ_{el}, on its surface (Fig. 10 *a′*). The larger σ_{el}^2 is, the more positive is the monolayer's spontaneous curvature (Kozlov et al. 1985, 1992; Lerche et al., 1987). Hence, the membrane spontaneous curvature is proportional to the difference of the charge densities squared of the two monolayers

$$J_S \sim \left[\left(\sigma_{el}^{out}\right)^2 - \left(\sigma_{el}^{in}\right)^2\right]. \tag{4}$$

Suppose that, due to the LEF-induced segregation of lipids, the charge density in the outer monolayer decreases, locally, to a value much smaller than that in the inner monolayer, $\left(\sigma_{el}^{out}\right)^2 \ll \left(\sigma_{el}^{in}\right)^2$. Then, according to Eq. 4, the membrane spontaneous curvature adopts a negative value, $J_S \sim -\left(\sigma_{el}^{in}\right)^2$, stimulating the inward bending (Fig. 10 *b′*) and, hence, membrane budding into an endocytic vesicle.

The modulus of the Gaussian curvature, $\bar{\kappa}$, determines the energy of change of membrane topology (see, e.g., Helfrich, 1990). For example, the energy change, accompanying the separation of a vesicle from the plasma membrane, has a contribution $4\pi \cdot \bar{\kappa}$, meaning that negative values of $\bar{\kappa}$ stimulate membrane fission involved in endocytosis. For a symmetric bilayer membrane its Gaussian modulus can be expressed through the Gaussian moduli, $\bar{\kappa}_m$ and spontaneous curvatures, J_S^m, of its monolayers (Helfrich and Rennschuh, 1990; Ljunggren and Eriksson, 1992; Templer et al., 1998; Schwarz and Gompper, 2001; Siegel and Kozlov, 2004)

$$\bar{\kappa} = 2 \times \bar{\kappa}_m - 4 \times \kappa_m \times J_s^m \times \delta \tag{5}$$

where κ_m is the monolayer bending modulus and δ is the monolayer thickness. As mentioned below, the monolayer spontaneous curvature J_S^m becomes more positive with growing surface charge density $\left(\sigma_{el}^m\right)^2$. Hence, according to Eq. 5, concentrating surface charge by electric field results in a negative contribution to the membrane Gaussian modulus (Eq. 5). Moreover, it can be also shown that the monolayer's Gaussian modulus $\bar{\kappa}_m$ becomes more negative with growing monolayer charge density $\left(\sigma_{el}^m\right)^2$. Even further, the conclusions above about the effects of the surface charge on the Gaussian modulus are also qualitatively correct for asymmetric membranes, although the expression for $\bar{\kappa}$ is more complicated in that case.

Altogether we conclude that asymmetric concentration of surface charge in membrane monolayers makes the local Gaussian modulus more negative and, hence, promotes membrane fission involved in generating an endocytic vesicle. The suggested mechanism is suitable for explaining the LEF-induced stimulation of both adsorptive and fluid-phase uptake (Antov et al., 2004).

Dependence of LEF-induced uptake on electrical field parameters

The dependence of uptake on the electrical parameters reflects the primary interaction of cells with the electric field.

The increase in LEF-induced BSA-FITC uptake on medium conductivity (Fig. 9 *A*) may hint at the uptake being dependent on the electric current flowing through the cell suspension. This, in turn, might indicate the possible involvement of electroosmosis in the LEF-stimulated uptake. These findings are in contrast to the uptake induced by high electric field pulses, where the uptake efficiency is either not altered by the ionic strength of the extracellular medium (Pucihar et al., 2001) or is higher in a low-conductive medium (Zimmermann et al., 2000). However, cellular viability was shown to be higher in a low-conductive medium (Pucihar et al. 2001; Zimmermann et al. 2000), similar to our findings. The quadratic dependence of the uptake on medium conductivity may reflect the complex character of LEF-induced uptake phenomena, where the overall uptake results from a multistage process, where each stage can be influenced by LEF.

The dependence of the uptake on electric field strength gave the best fit for a quadratic dependence (coefficient of determination of 0.98, as compared with a lower value of 0.92 for a linear regression). The lateral segregation of charged membrane components, leading to local changes in surface charge density, depends linearly on electric field. Thus, it may be suggested that the quadratic dependence of uptake on electric field emerges from the dependence of changes of the spontaneous membrane curvature on the difference in the charge densities squared between the two monolayers (Eq. 4).

Contrary to the uptake via electroporation-based mechanism, which is induced by high electric field pulses, LEF-induced uptake shows no signs of threshold values of the electric field strength. It is of interest that a threshold value of $\sim$100 μs can be detected for the pulse duration (Fig. 9 *B*), corresponding to a duty cycle of 5%. This may be attributed to the diffusional relaxation process of charged lipids or proteins during the ''off'' period, which can diminish the field-induced segregation. A threshold value of 20% duty cycle was found for the induced migration of concanavalin A receptors on the cell surface by pulsed electric fields, though different cell lines and electric field conditions were employed (Lin-Liu et al., 1984).

The linear decline of viability of cells exposed to LEF with increased conductance (Fig. 9 *D*) probably reflects cytotoxic effects of electrolysis products. The amount of these products is expected to be proportional to the total current (charge) passing through the sample. Viability of COS 5-7 cells, exposed to LEF of 20 V/cm decreased linearly down to 85% upon lengthening pulse duration to 250 μs (Fig. 9 *F*). At the same time, viability of cells decreased down to 73% when electric field strength increased to 43 V/cm.

In conclusion, this study demonstrates that exposure of cell suspension to a train of low-pulsed electric fields, which is shorter than the rotational relaxation time of the cells, leads to changes in the cell surface that bring about an increased specific and nonspecific adsorption of BSA as well as leading to cellular aggregation. These surface changes, which are temperature-independent, are followed by a temperature-dependent internalization of the adsorbed macromolecules through endocytic pathway(s). It is suggested that these two processes are initiated by electrophoretic-induced segregation of charged membrane components in the outer monolayer of the plasma membrane leading to asymmetric charge density between the outer and inner monolayer of the plasma membrane, promoting local changes both in the spontaneous curvature and the Gaussian modulus, hence leading to membrane bending toward the inside of the cell and to membrane fission involved in generation of an endocytic vesicle.

We thank Michael Kozlov for fruitful discussions, especially on the effects of membrane surface charge alterations on membrane elastic properties. This work was carried out in partial fulfillment of a PhD requirement of Y. Antov.

This study was supported by the Israel Science Foundation founded by the Israel Academy of Sciences and Humanities (grant 1029/03 to R.K.).

REFERENCES

Adair, R. K. 1999. Effects of very weak magnetic fields on radical pair reformation. *Bioelectromagnetics*. 20:255–263.

Ahlbom, A., E. Cardis, A. Green, M. Linet, D. Savitz, and A. Swerdlow. 2001. Review of the epidemiologic literature on EMF and health. *Environ. Health Perspect.* 109:911–933.

Antov, Y., A. Barbul, and R. Korenstein. 2004. Electroendocytosis: stimulation of adsorptive and fluid-phase uptake by pulsed low electric fields. *Exp. Cell Res.* 297:348–362.

Asawakarn, T., J. Cladera, and P. O'Shea. 2001. Effects of the membrane dipole potential on the interaction of saquinavir with phospholipid membranes and plasma membrane receptors of Caco-2 cells. *J. Biol. Chem.* 276:38457–38463.

Birn, H., J. C. Fyfe, C. Jacobsen, F. Mounier, P. J. Verroust, H. Orskov, T. E. Willnow, S. K. Moestrup, and E. I. Christensen. 2000. Cubilin is an albumin binding protein important for renal tubular albumin reabsorption. *J. Clin. Invest.* 105:1353–1361.

Borgens, R. B., J. W. Vanable, Jr., and L. F. Jaffe. 1977. Bioelectricity and regeneration: large currents leave the stumps of regenerating newt limbs. *Proc. Natl. Acad. Sci. USA*. 74:4528–4532.

Brumfeld, V., I. R. Miller, and R. Korenstein. 1989. Electric field-induced lateral mobility of Photosystem I in the photosynthetic membrane: a study by electrophotoluminescence *Biophys. J.* 56:607–614.

Chen, Y. D., and T. Y. Tsong. 1994. On the efficiency and reversibility of active ligand transport induced by alternating rectangular electric pulses. *Biophys. J.* 66:2151–2158.

Chernomordik, L. V., D. Papahadjopoulos, and T. Y. Tsong. 1991. Increased binding of liposomes to cells by electric treatment. *Biochim. Biophys. Acta*. 107:193–197.

Christensen, E. I., and H. Birn. 2002. Megalin and cubilin: multifunctional endocytic receptors. *Nat. Rev. Mol. Cell Biol.* 3:256–266.

Farkas, D. L., R. Korenstein, and S. Malkin. 1984. Electrophotoluminescence and the electrical properties of the photosynthetic membrane. I: initial kinetics and the charging capacitance of the membrane. *Biophys. J.* 45:363–373.

Foster, K. R. 2003. Mechanisms of interaction of extremely low frequency electric fields and biological systems. *Radiat. Prot. Dosimetry*. 106:301–310.

Gehl, J. 2003. Electroporation: theory and methods, perspectives for drug delivery, gene therapy and research. *Acta Physiol. Scand.* 177: 437–447.

Gekle, M., S. Mildenberger, R. Freudinger, and S. Silbernagl. 1996. Functional characterization of albumin binding to the apical membrane of OK cells. *Am. J. Physiol.* 271:F289–F291.

Glogauer, M., and C. A. McCulloch. 1992. Introduction of large molecules into viable fibroblasts by electroporation: optimization of loading and identification of labeled cellular compartments. *Exp. Cell Res.* 200:227–234.

Golzio, M., J. Teissie, and M. P. Rols. 2002. Direct visualization at the single-cell level of electrically mediated gene delivery. *Proc. Natl. Acad. Sci. USA.* 99:1292–1297.

Groves, J. T., S. G. Boxer, and H. M. McConnell. 1997. Electric field-induced reorganization of two-component supported bilayer membranes. *Proc. Natl. Acad. Sci. USA.* 94:13390–13395.

Groves, J. T., S. G. Boxer, and H. M. McConnell. 1998. Electric field-induced critical demixing in lipid bilayer membranes. *Proc. Natl. Acad. Sci. USA.* 95:935–938.

Hamilton, J. A. 2002. How fatty acids bind to proteins: the inside story from protein structures. *Prostaglandins Leukot Essent Fatty Acids.* 67: 65–72.

Helfrich, W. 1973. Elastic properties of lipid bilayers: theory and possible experiments. *Z. Naturforsch.* 28:693–703.

Helfrich, W. 1990. Elasticity and thermal undulations of fluid films of amphiphiles. *In* Les Houches, 1988—Liquids at Interfaces. J. Charvolin, J.-F. Joanny, and J. Zinn-Justin, editors. Elsevier Science Publishers, Oxford, UK. 212–237.

Helfrich, W., and H. Rennschuh. 1990. Landau theory of the lamellar-to-cubic phase transition. *J. Phys. (Paris) Colloq.* 51:189–195.

Jaffe, L. F. 1966. Electrical currents through the developing fucus egg. *Proc. Natl. Acad. Sci. USA.* 56:1102–1109.

Jaffe, L. F. 1977. Electrophoresis along cell membranes. *Nature.* 265:600–602.

Kinosita, K., Jr., and T. Y. Tsong. 1977. Formation and resealing of pores of controlled sizes in human erythrocyte membrane. *Nature.* 268:438–441.

Kozlov, M. M., D. Lerche, and V. S. Markin. 1985. Free energy and spontaneous curvature of charged membrane with glycocalix. *Biologicheskie Membrany.* 2:806–812.

Kozlov, M. M., M. Winterhalter, and D. Lerche. 1992. Elastic properties of strongly curved interfaces. Effect of electric surface charge. *J. Phys. II. France.* 2:175–185.

Lacy-Hulbert, A., J. C. Metcalfe, and R. Hesketh. 1998. Biological responses to electromagnetic fields. *FASEB J.* 12:395–420.

Lerche, D., M. M. Kozlov, and V. S. Markin. 1987. Electrostatic free energy and spontaneous curvature of spherical charged layered membrane. *Biorheology.* 24:23–34.

Lin-Liu, S., W. R. Adey, and M. M. Poo. 1984. Migration of cell surface concanavalin A receptors in pulsed electric fields. *Biophys. J.* 45:1211–1217.

Ljunggren, S., and J. C. Eriksson . 1992. Minimal surfaces and Winsor III microemulsions. *Langmuir.* 8:1300–1306.

Lund, K., L. Opresko, C. Starbuck, B. Walsh, and H. Wiley. 1990. Quantitative analysis of the endocytic system involved in hormone-induced receptor internalization. *J. Biol. Chem.* 265:15713–15723.

Mamdouh, Z., M. C. Giocondi, R. Laprade, and C. Le Grimellec. 1996. Temperature dependence of endocytosis in renal epithelial cells in culture. *Biochim. Biophys. Acta.* 1282:171–173.

Martins, M. C. L., B. D. Ratner, and M. A. Barbosa. 2003. Protein adsorption on mixtures of hydroxyl- and methyl-terminated alkanethiols in self-assembled monolavers. *J. Biomed. Mater. Res.* 67:158–171.

McLaughlin, S., and M. M. Poo. 1981. The role of electro-osmosis in the electric-field-induced movement of charged macromolecules on the surfaces of cells. *Biophys. J.* 34:85–93.

McLean, M. R., and L. L. Hause. 1981. Collagen-induced platelet aggregation as studies by electronic particle size analysis. *Thromb. Haemost.* 46:731–733.

Miller, I. R., V. Brumfeld, and R. Korenstein. 1994. Conformation and mobility of membrane proteins in electric fields. *In* Advances in Chemistry Series, Vol. 235. Membrane Electrochemistry. I. Vodyanoy and M. Blank, editors. Oxford University Press, Oxford, UK. 107–127.

Neumann, E., and K. Rosenheck. 1972. Permeability changes induced by electric impulses in vesicular membranes. *J. Membr. Biol.* 10:279–290.

Nuccitelli, R. 2003. Endogenous electric fields in embryos during development, regeneration and wound healing. *Radiat. Prot. Dosimetry.* 106:375–383.

Nuccitelli, R., and L. F. Jaffe. 1974. Spontaneous current pulses through developing fucoid eggs. *Proc. Natl. Acad. Sci. USA.* 71:4855–4859.

Orida, N., and M. M. Poo. 1978. Electrophoretic movement and localisation of acetylcholine receptors in the embryonic muscle cell membrane. *Nature.* 275:31–35.

O'Shea, P. 2003. Intermolecular interactions with/within cell membranes and the trinity of membrane potentials: kinetics and imaging. *Biochem. Soc. Trans.* 31:990–996.

Poo, M. M. 1981. In situ electrophoresis of membrane components. *Annu. Rev. Biophys. Bioeng.* 10:245–276.

Poo, M. M., J. W. Lam, and N. Orida. 1979. Electrophoresis and diffusion in the plane of the cell membrane. *Biophys. J.* 26:1–22.

Poo, M. M., and K. R. Robinson. 1977. Electrophoresis of concanavalin A receptors along embryonic muscle cell membrane. *Nature.* 265:602–605.

Pucihar, G., T. Kotnik, M. Kanduser, and D. Miklavcic. 2001. The influence of medium conductivity on electropermeabilization and survival of cells in vitro. *Bioelectrochemistry.* 54:107–115.

Radhakrishnan, A., and H. M. McConnell. 2000. Electric field effect on cholesterol-phospholipid complexes. *Proc. Natl. Acad. Sci. USA.* 97: 1073–1078.

Rosemberg, Y., and R. Korenstein. 1997. Incorporation of macromolecules into cells and vesicles by low electric fields: induction of endocytic-like processes. *Bioelectrochem. Bioenerg.* 42:275–281.

Schnitzer, J. E., and J. Bravo. 1993. High-affinity binding, endocytosis, and degradation of conformationally modified albumins: potential role of gp30 and gp18 as novel scavenger receptors. *J. Biol. Chem.* 268:7562–7570.

Schwan, H. P. 1957. Electrical properties I tissue and cell suspensions. *Adv. Biol. Med. Phys.* 5:147–209.

Schwarz, U. S., and G. Gompper. 2001. Bending frustration of lipid-water mesophases based on cubic minimal surfaces. *Langmuir.* 17:2084–2096.

Siegel, D. P., and M. M. Kozlov. 2004. The Gaussian curvature elastic modulus of N-monomethylated dioleoylphosphatidylethanolamine: relevance to membrane fusion and lipid phase behavior. *Biophys. J.* 87:366–374.

Sowers, A. E., and C. R. Hackenbrock. 1981. Rate of lateral diffusion of intramembrane molecules: measurement by electrophoretic displacement and rerandomization. *Proc. Natl. Acad. Sci. USA.* 78:6246–6250.

Song, B., M. Zhao, J. V. Forrester, and C. D. McCaig. 2002. Electrical cues regulate the orientation and frequency of cell division and the rate of wound healing in vivo. *Proc. Natl. Acad. Sci. USA.* 99:13577–13582.

Sprague, E. A., J. L. Kelley, C. A. Suenram, A. J. Valente, M. Abreu-Macomber, and C. J. Schwartz. 1985. Stimulation of albumin endocytosis by cationized ferritin in cultured aortic smooth-muscle cells. *Am. J. Pathol.* 121:433–443.

Teissie, J. 2002. Membrane destabilizations supporting electropermeabilization. *Cell Mol. Biol. Lett.* 7:96–100.

Templer, R. H., B. J. Khoo, and J. M. Seddon. 1998. Gaussian curvature modulus of an amphiphile monolayer. *Langmuir.* 14:7427–7434.

Tiruppathi, C., W. Song, M. Bergenfeldt, P. Sass, and A. B. Malik. 1997. Gp60 activation mediates albumin transcytosis in endothelial cells by tyrosine kinase-dependent pathway. *J. Biol. Chem.* 272:25968–25975.

Tsong, T. Y. 2002. Na,K-ATPase as a brownian motor: electric field-induced conformational fluctuation leads to uphill pumping of cation in the absence of ATP. *J. Biol. Phys.* 28:309–325.

Wang, E. T., Y. L. Yin, M. Zhao, J. V. Forrester, and C. D. McCaig. 2003. Physiological electric fields control the G(1)/S phase cell cycle checkpoint to inhibit endothelial cell proliferation. *FASEB J.* 17:458–460.

Weaver, J. C. 2003. Electroporation of biological membranes from multicellular to nano scales. *IEEE Trans. Dielectr. Electr. Insul.* 10:754–768.

Weaver, J. C., T. E. Vaughan, and R. D. Astumian, 2000. Biological sensing of small field differences by magnetically sensitive chemical reactions. *Nature.* 405:707–709.

Weaver, J. C., T. E. Vaughan, and G. T. Martin. 1999. Biological effects due to weak electric and magnetic fields: The temperature variation threshold. *Biophys. J.* 76:3026–3030.

Wiley, H. 1988. Anomalous binding of epidermal growth-factor to A431 cells is due to the effect of high receptor densities and a saturable endocytic system. *J. Cell Biol.* 107:801–810.

Xie, T. D., Y. D. Chen, P. Marszalek, and T. Y. Tsong. 1997. Fluctuation-driven directional flow in biochemical cycle: further study of electric activation of Na/K pumps. *Biophys. J.* 72:2496–2502.

Yammani, R. R., M. Sharma, S. Seetharam, J. E. Moulder, N. M. Dahms, and B. Seetharam. 2002. Loss of albumin and megalin binding to renal cubilin in rats results in albuminuria after total body irradiation. *Am. J. Physiol. Regul. Integr. Comp. Physiol.* 283:R339–R346.

Ying, P. Q., Y. Yu, G. Jin, and Z. L. Tao. 2003. Competitive protein adsorption studied with atomic force microscopy and imaging ellipsometry. *Colloids Surfaces B.* 32:1–10.

Yokoyama, S., T. Takeda, T. Tsunoda, Y. Ohta, T. Imura, and M. Abe. 2002. Membrane properties of mixed dipalmitoylphosphatidylglycerol/ganglioside G(M3) liposomes in the presence of bovine serum albumin. *Colloid Surface B.* 27:141–146.

Zhao, M., A. Dick, J. V. Forrester, and C. D. McCaig. 1999. Electric field-directed cell motility involves up-regulated expression and asymmetric redistribution of the epidermal growth factor receptors and is enhanced by fibronectin and laminin. *Mol. Biol. Cell.* 10:1259–1276.

Zhao, M., J. Pu, J. V. Forrester, and C. D. McCaig. 2002. Membrane lipids, EGF receptors, and intracellular signals colocalize and are polarized in epithelial cells moving directionally in a physiological electric field. *FASEB J.* 16:857–859.

Zimmermann, U., U. Friedrich, H. Mussauer, P. Gessner, K. Hamel, and V. Sukhorukov. 2000. Electromanipulation of mammalian cells: fundamentals and application. *IEEE Trans. Plasma Sci.* 28:72–82.

Zimmermann, U., G. Pilwat, and F. Riemann. 1974. Dielectric breakdown of cell membranes. *Biophys. J.* 14:881–899.